Development and Validation of a Tool for In-Plane Antilock Braking System (ABS) Simulations

Karan Rajiv Khanse

Thesis submitted to the faculty of the Virginia Polytechnic Institute and State University in partial fulfillment of the requirements for the degree of

Master of Science
In
Mechanical Engineering

Saied Taheri (Chair)

Corina Sandu

Ronald Kennedy

July 9th, 2015

Blacksburg, VA

Keywords: Vehicle Model, CarSim, Tire Model, Rigid Ring, ABS

Development and Validation of a Tool for In-Plane Antilock Braking System (ABS) Simulations

Karan Rajiv Khanse

ABSTRACT

Automotive and Tire companies spend extensive amounts of time and money to tune their products through prototype testing at dedicated test facilities. This is mainly due to the limitations in the simulation capabilities that exist today. With greater competence in simulation, comes more control over designs in the initial stages, which in turn lowers the demand on the expensive stage of tuning. The work presented, aims at taking today's simulation capabilities a step forward by integrating models that are best developed in different software interfaces. An in-plane rigid ring model is used to understand the transient response of tires to various high frequency events such as Anti-Lock Braking and short wavelength road disturbances. A rule based ABS model performs the high frequency braking operation. The tire and ABS models have been created in the Matlab-Simulink environment. The vehicle model has been developed in CarSim. The models developed in Simulink have been integrated with the vehicle model in CarSim, in the form of a design tool that can be used by tire as well as vehicle designers for further tuning of the vehicle functional performances as they relate to in-line braking scenarios. Outdoor validation tests were performed to obtain data from a vehicle that was measured on a suspension parameter measuring machine (SPMM) in order to complement this design tool. The results of the objective tests performed have been discussed and the correlations and variations with respect to the simulation results have been analyzed.

ACKNOWLEDGEMENTS

I would like to deeply thank my academic advisor Dr. Saied Taheri for giving me the opportunity to work on this project at the Center for Tire Research (CenTiRe). His constant advice played a huge role in the completion of my thesis.

I would also like to thank Dr. Corina Sandu and Dr. Ronald Kennedy for their participation in my thesis committee.

Finally, I would like to acknowledge the industry mentors, especially Goodyear, Bridgestone, Hankook, Apollo, GITI, Toyo, Mitsubishi, Yokohama, MRF and Honda at the Center for Tire Research (CenTiRe), whose valuable comments and feedback steered the project in the right direction.

TABLE OF CONTENTS

List of Figures:

List of Tables:

Chapter 1:

Introduction and Background

Active safety is an important phenomenon designed into vehicles in an effort to mitigate the risks that are posed due to unpredictable environmental factors or unsafe driving. This is a highly multi-disciplinary field and involves measures being taken from a large number of industries simultaneously; the tire industry being an important one. With the rapid improvements in computational capabilities over the past two decades, more and more efforts are being made to utilize the power of computation and physically modeled systems in order to improve the utility value and cost effectiveness of a particular product. For the work being presented here, tires are being used as a tool to enable improvements to the active safety from the point of view of vehicular braking. Modeling of tires is considered to be a major challenge due to the high level of complexity that comes on account of multiple structures within the tire. A number of advanced models have been developed over the years to predict the dynamic response of tires under different operating conditions.

The following sections in the current chapter explain assessments that are traditionally made while developing a braking system and the natural lead to antilock braking systems due to limitations in conventional braking systems. With a brief summary of antilock braking systems, the motivation and objectives of this research are outlined, followed by the background study involved in this work. Chapter 2 explains the mathematical models that were used to simulate the different systems

involved. The techniques used to integrate these models to work together as a simulation tool have been explained in Chapter 3. Chapter 4 discusses the results that were obtained from the simulation tool and its conformance with validation test data. Chapter 5 concludes this thesis with a summary of the work done.

1.1 Introduction to Braking Assessments

Designing the braking system of an automobile is an iterative process, like most other systems on the vehicle. Designs are first implemented on the vehicle in the form of prototypes. These systems are then tested for their functionality under various scenarios that the vehicle could possibly come across in its lifetime. Systems are tuned based on the gap between its existing performance and the performance targets that are set during the design phase. The existing performance of a system is judged based on a two-fold approach: Subjective Assessments and Objective Evaluations.

Subjective Assessments involve an expert driver driving the vehicle and performing various maneuvers. Assessments are then made by the expert driver in the form of comments and ratings. Comments such as - 'Vehicle pulling to side during straight ahead braking ...' or 'Confidence low while braking in turn …' help identify potential problem areas in the system. Further, subjective rating sheets are a way to compare the vehicle performance under different set-ups. For example, ratings are given for a particular braking scenario using different tires. The cumulative ratings from multiple drivers eventually help finalizing a particular set-up for the vehicle.

Objective evaluations complement subjective assessments. They communicate the actual performance of the vehicle to the designers in an engineering language. Results from these tests usually form hard numbers that can be readily compared to

judge a better performance. They usually require expensive equipment to measure these entities. An example of an objective braking assessment would be the distance covered by the vehicle under maximum braking potential. In order to evaluate this, the maximum braking force can be measured and so on. This method of evaluation helps in identifying the weak link when the goal is to improve a system performance. With some experience, subjective assessments are usually correlated to objective metrics, which can be measured during objective evaluations in order to quantify the source of a positive or negative subjective assessment.

In the broader sense, the objective of a braking system is to break the speed of the vehicle as fast as possible. The application, in most scenarios includes avoiding collision with an object in the path of a vehicle. The objective of braking quickly, remains important even when less critical braking applications are considered which do not involve obstacle avoidance. Race cars, for example, have a sole objective of reducing lap times. While accelerating faster is the way to reduce lap times, when the vehicle spends less time in braking before corners, it leaves more time and scope for the vehicle to accelerate and in turn reduce lap times. The only way to reduce time spent under braking is to brake the vehicle harder without losing the stability of the vehicle. This goal of braking harder can be quantified into a number of subjective evaluations and objective metrics as are described here [1].

Braking Quickness:

The first and the most important measure of braking is braking quickness. The term “braking quickness” is a subjective attribute used by the driver to express how fast the vehicle brakes. Braking is said to begin after the driver has spent time in reacting to the obstacle that s/he sees in the path of the vehicle. While reaction times can be minimized when the driver is in a state of alertness, it cannot be eliminated

completely. As soon as the driver slams on the brakes, there is a certain time interval between this instant and when the maximum braking force is generated. The speed at which the driver applies force on the pedal has a great influence on this time. For a vehicle with no ECU intervention technologies, the driver needs to maintain a balance between a controlled build-of braking force and aggressiveness to avoid wheel lock ups. After the maximum braking force has been developed, the vehicle sustains this level of braking until it comes to a complete stop or to a desired low speed. Braking quickness can then be quantified in terms of the time required from brake application to the vehicle stopping or the distance covered between the same points. Figure 1.1 summarizes this motion of braking.

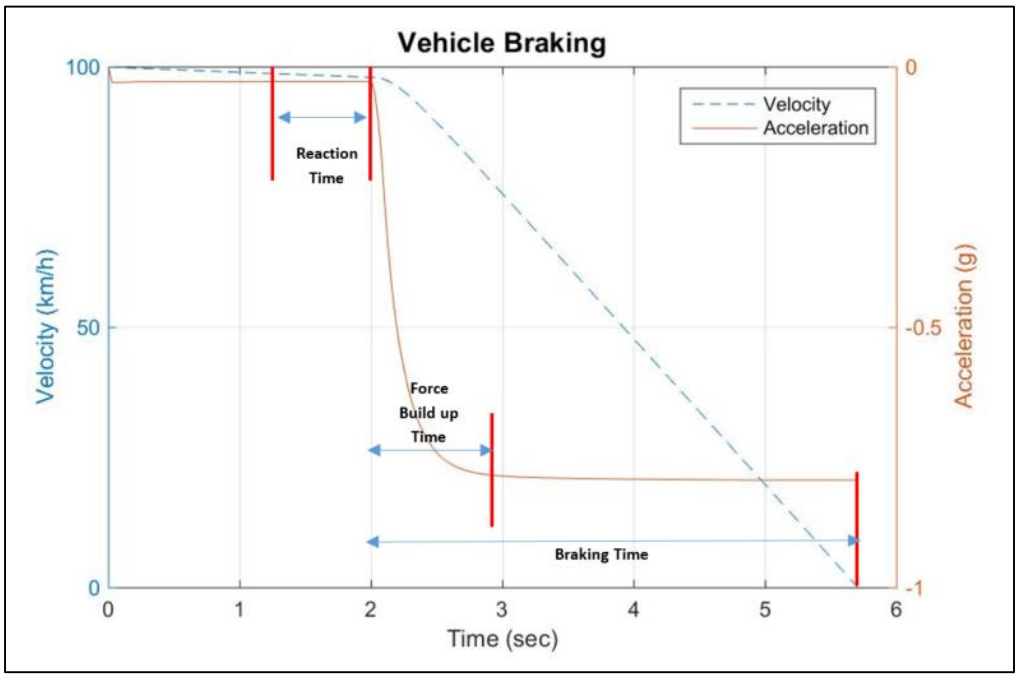

Figure 1.1: Braking of a Vehicle

Braking Points: This metric is a direct product of the previously discussed metric of braking quickness. It finds its application mainly in the field of race car engineering. Braking points are defined as the latest physical location on the track where the driver is forced to apply brakes ahead of an approaching turn. This point is largely

dependent on the approach speed of the vehicle as it affects the reference point that the driver uses to start braking, in following a particular race line. However, they are also a direct result of the confidence that the driver has on the vehicle's braking system. The quicker the system can slow the vehicle down, the later can the driver brake, making him faster around the circuit. This is considered as a secondary metric as it is a direct product of braking distance.

Brake Effort:

This metric quantifies the amount of effort applied by the driver on the brake pedal. The force applied by the driver on the pedal is transferred into hydraulic energy that is transferred through the incompressible fluids in the hydraulic lines all the way to the brake pads, which are eventually responsible for braking the discs or drums depending on the application. The effort felt by the driver is a result of the hydraulic and mechanical design of the brake system. This design and in turn the effort directly affects the ability of the driver to brake the vehicle at its maximum potential. Extremely high efforts reduce the speed at which the driver can press the pedal as well as the maximum level to which the brakes are applied.

Pedal Travel:

Repeated and prolonged use of the braking system causes the brake pads to wear out and become ineffective. Data obtained by measuring pedal travel from the initial to the furthest pedal position under maximum braking potential gives insight into wear of the brake pads. Further, a system designed to have a greater pedal travel can affect the ability of the system to quickly generate the maximum braking force. Greater overall pedal travels require drivers to spend more time in reaching the furthest pedal position thereby taking more time in the build-up of maximum acceleration levels.

Brake Temperatures:

Selection of materials for brake pads and brake discs determine the temperature build-up that will occur for a particular braking scenario due to the friction between them. Based on this temperature build-up, a particular system is set-up for a designed maximum working temperature. If operating temperatures exceed this threshold, it usually results in a reduced brake effectiveness.

Brake Lock-ups:

In order to understand wheel lock-up occurrences during braking operations, it is important to understand the concept of a longitudinal slip ratio. For a vehicle being driven along the road, its velocity is identical to that of its own wheels. When brakes are applied to the vehicle, the speed of the wheels reduces as compared to the vehicle that continues to move under its own inertia. Longitudinal slip ratio is a representation that is used to quantify this difference in velocities. It can be calculated using the following formulation:

$$\kappa = \frac{V - v}{v} \times 100$$

Where, κ - is the longitudinal wheel slip (%)

V - is the velocity of the vehicle (m/s)

v - Linear velocity of the wheels (m/s)

Longitudinal slip ratios also arise for the case of accelerating wheels on surfaces with limited traction. This is the case where wheel speeds are higher than the vehicle speed and hence are represented by an opposite sign as that for the case of braking. A longitudinal slip ratio value of 0 indicates a case where the wheel has the same linear velocity as that of the longitudinal velocity of the vehicle. Whereas, a value

of 1 indicates the wheel has no velocity when the vehicle is still under longitudinal motion. This case were the slip ratio reaches 1 is when the vehicle is said to have its wheels locked up. Excessive wheel lock-ups usually cause a lot of uneven tire wear, which results in an unpleasant ride. Brake lock-ups are usually partial and are not seen on all wheels simultaneously. They occur on wheels with the least amount of load on them as well as on the axle with a greater brake bias. Wheel lock-ups can easily be detected using wheel speed channels as near vertical drops when plotted against time.

Brake Balance:

Brake balance can be defined as the distribution between the front and rear brake line pressures. Primarily, brake pressures depend on the diameter of the master cylinder and the position of the brake balance bar in cases where they exist. Brake balance can be quantified by either front or rear brake bias and is calculated using the formula:

$$BrakeBias_{front} = \frac{P_f}{P_f + P_r} \times 100$$

Where, P_f - Front brake pressure

P_r - Rear brake pressure

The decision of selecting a particular brake bias value for a given vehicle is dependent on a number of factors. Traction can be understood as the amount of longitudinal force that can be generated at the tire contact patch. This is the force that aids a vehicle to either accelerate or decelerate. The amount of traction available for a given tire-road interface is dependent on the coefficient of friction between that

particular tire compound and road surface, as well as the normal load on that wheel. This can be seen in the formula for friction, which can be given by:

$$\mu = \frac{F_f}{F_n}$$

Where, μ - Coefficient of friction

F_f - Frictional force

F_n - Normal Force

Thus, the greater the coefficient of friction, greater is the traction available. This is the reason why wheel slips during acceleration and deceleration are seen more on icy roads as compared to dry roads.

It can also be seen that the frictional force is directly proportional to the normal load. Hence, for a consistent tire-road combination, on an all-wheel drive vehicle, the axle with the greater load on it is capable of generating greater longitudinal forces. For a given traction capability of a vehicle, it is the job of the braking system to extract the greatest braking forces from it. This is done by setting the brake balance of the vehicle proportional to the traction available on its wheels.

1.2 Antilock Braking Systems (ABS)

The problem imposed by braking wheel lock-ups is not limited simply to tire-wear as seen earlier. Its more profound effects relate to traction at the tire-road interface. The following is a discussion of the relationship of wheel slip with traction.

Figure 1.2 shows the variation of longitudinal slip ratio of a wheel plotted against the longitudinal force for a particular tire under braking as illustrated by Zegelaar [2].

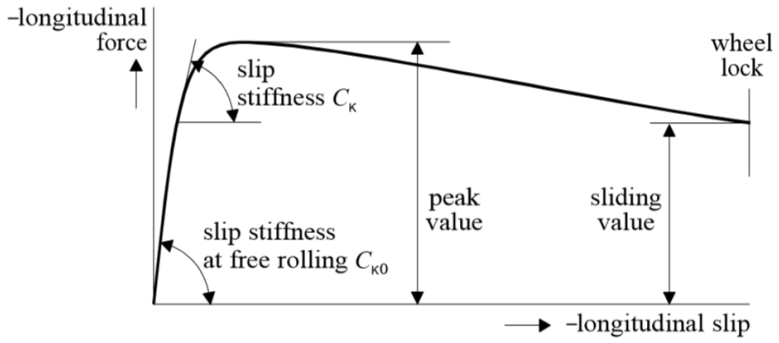

Figure 1.2: Longitudinal Slip Ratio vs Braking Force [2]-
Peter W.A. Zegelaar, 'The dynamic response of tires to brake torque variations and road unevenness', Ph.D. thesis, Delft University of Technology, Netherlands, 1998. Used under fair use 2015.

It can be seen that longitudinal force has a linear relationship with slip ratio up to a range of 10-15%. After peaking, the force starts dropping off gradually at higher slip ratios. The best braking performance can be extracted from a tire-vehicle combination when this braking force is maintained at the peak region of this plot, which means- when it is maintained at a particular slip ratio. This highly important function is performed by the antilock braking systems (ABS), the main advantages of which include- reducing stopping distance on dry, wet or icy roads, as well as maintaining steering control while braking. Both these functions being extremely important in the event of extreme road situations.

Braking System:

Figure 1.3 shows the schematic of a conventional braking system with a dual diagonal system design. The front wheels typically employ disc brakes whereas the rear wheels employ drum brakes, both of which work on the principle of heat

dissipation. The brake pedal as operated mechanically by the driver is connected to the master cylinder through a vacuum booster. The master cylinder is responsible for creating pressure in the hydraulic system. This hydraulic pressure reaching the calipers or wheel cylinders is used to mechanically apply the brakes. The vacuum booster which utilizes engine vacuum, the hydraulics as well as the mechanical ratio of the pedal make it possible to brake the entire vehicle from forces that arise from a human foot effort.

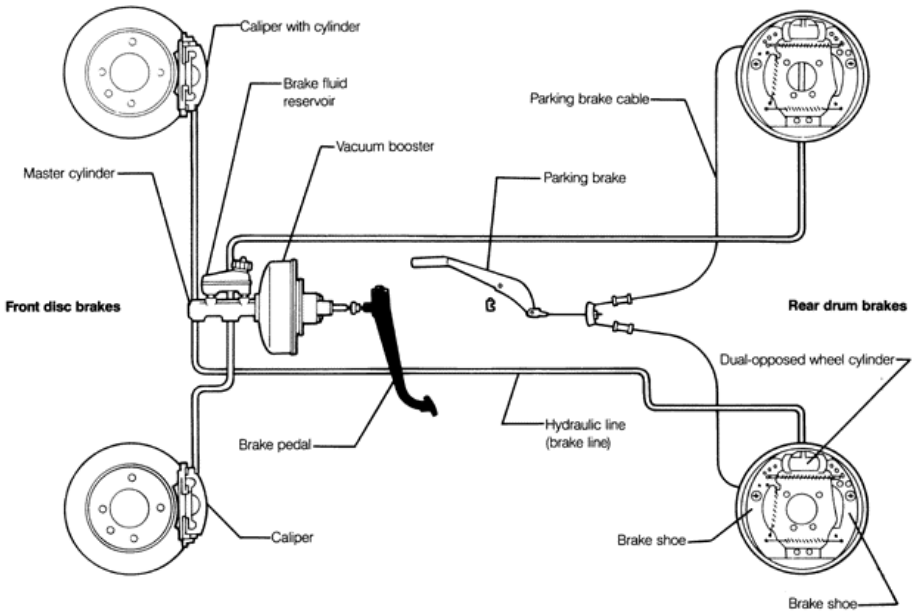

Figure 1.3: Conventional Braking System

The antilock braking system, in addition to the above described components consists of 3 major components:

1) Wheel speed sensors (WSS): Typically, WSSs work with the help of electromagnetic or Hall-effect pulse pick-ups with toothed wheels. These toothed wheels are directly mounted on either the wheel hubs or the drive shafts for those wheels. The toothed wheel generates an AC voltage as it

rotates. The voltage frequency is directly proportional to the wheel's rotational speed.

2) Electronic Control Unit (ECU): The ECU is responsible for amplifying and filtering the signals that are received form the sensors. The slip at each wheel is calculated by comparing the speed of the individual wheels with the reference speed of the vehicle. Wheel accelerations and wheel slip values are used by the ECU to detect a wheel lock-up or a condition that could lead to a lock-up.
3) Hydraulic pressure modulator: Based on the detections made by the ECU of lock-ups or impending lock-ups, the hydraulic pressure modulator, and electro-hydraulic device, is responsible for reducing, holding and restoring the pressure of the wheel brakes by manipulating solenoid valves. It tends to serve as a link between the brake master cylinder and wheel brake cylinders.

The main challenges in the design of an ABS control arise from the high level of non-linearity and uncertainty of the problem. It is, at times difficult to solve the problem using classical linear frequency domain methods. Further, the following enumerates the challenges faced while designing this controller:

1) The controller must operate at an unstable equilibrium point for optimal performance
2) Coefficients of friction on the brake pad-brake disc interface changes with temperature
3) The tire slip ratio varies widely and rapidly on rough roads due to tire bounce
4) There is a high level of noise and uncertainty involved with the tire slippage signals, accurate signals from which are important for controller performance
5) Maximum braking force varies over a wide range depending on road conditions

6) Transport delays within the braking system limit the bandwidth of the control system

1.3 Research Motive

With the knowledge of the importance of antilock braking as safety systems in today's automobile, the industry has directed a good amount of effort towards having a deeper understanding of all the factors that influence it. Although braking algorithms and braking system components have a primary influence on the braking performance of a given tire-vehicle combination, they are not the only factors that determine its performance.

Vehicle manufacturers usually turn to tires for optimizing braking performance too as part of its subjective/objective evaluation, since the longitudinal forces required for braking are primarily developed at the contact patch of the tire. Further, as part of aftermarket sales, consumers tend to rely widely on magazine reviews over purchase of new tires, where braking performance is an important assessment parameter.

Significant efforts by Zegelaar [2], and also previously at the Center for Tire Research by Srikanth [3] have been made in modeling tires for the high frequency vibrations occurring from Antilock Braking Systems (ABS). Srikanth integrated the developed in-plane tire model with a quarter car model for its performance studies. As a continuation to the same work at the center, there was a thrust from the industry to be able to predict the performance for the more relevant application of full vehicles.

Having a model that is able to predict braking performances accurately considering tire dynamics implies an understanding of the influence of tire parameters on braking performance. A better understanding implies a better control over the parameters, which can eventually be used to improve braking performance by performing a design of experiment of the different parameters involved.

1.4 Objectives of the Research

With a clear motivation, the following objectives were established for the research:

- To develop a simulation tool that is capable of predicting the antilock braking performances of the vehicle accurately.
- To utilize a tire model developed in Matlab/Simulink, that is capable of analyzing the dynamic performance of tires at frequency excitations up to 100Hz that arise from antilock braking fluctuations as well as short wavelength disturbances from the unevenness of roads.
- To use industry accepted standard formats for tire parameter implementation in the tire models.
- To utilize a Matlab/Simulink model for the antilock braking system which is comparable to the systems fitted on commercial vehicles in terms of its control algorithms, torque applications and frequency of pressure modulations.
- To adapt the tire and ABS models developed previously for a quarter car application, so that they can be integrated with accurate full-vehicle models.
- To simplify implementation of real vehicle data into the vehicle model and to ease the vehicle parameterization procedure.
- To validate the performances predicted by the simulation tool with the help of outdoor tests

- To ensure that the simulation tool is not computationally expensive as compared to other platforms such as Finite Element Methods (FEM).

1.5 Background on Modeling

1.5.1 Tires

1.5.1.1 The Pneumatic Tire

Consisting of 20 or more components made from 15 or more rubber compounds, the pneumatic tire is one of the most complex components of today's automobile since it was first introduced in the late 1800s. With a high level of engineering, these structural composites are made to meet requirements from the vehicle manufacturers in addition to the quality and performance expectations of the customer.

1. The primary function of the tire is to provide an interface between the vehicle and the road.
2. In addition, it is also responsible for supporting the load of the vehicle. The vehicle load causes the tire to deflect until the average contact area pressure is balanced by the tire's internal air pressure [4]. For a tire that is inflated to a pressure of 30psi, a 300lb load would require an average of 10sq. in. of contact area to support the load. A greater contact area or higher tire pressure are required for larger loads. Industry standards exist for loading conditions on tires as outlined in [4].
3. Friction between the tire and road is responsible for making the vehicle stop, start and turn corners as desired with dry asphalt providing the greatest coefficient of friction as compared to ice, or asphalt with a film of water on it.

Tread grooves designed into tires assist in reducing the water between the interface and thereby maintaining a safe amount of traction to drive over.

4. A key attribute to the pneumatic tire is its absorption of road irregularities. It acts as a spring and damper system to absorb impacts and road unevenness under a wide range of operating conditions thereby helping provide a superior ride to the vehicle passengers.

In addition to the basic functions described above, the tire is also expected to fulfil certain performance criteria as described below [4]:

1. Handling: It is the response of the vehicle to various driver control inputs. Tires being responsible for transferring forces and moments to the vehicle, are evaluated for their stability, linearity, on-center feel, response, recovery, etc. A number of tests are designed to evaluate these on the test-track.
2. Ride Comfort: A vehicle's ride quality is responsible for the comfort levels as felt by the occupants of the vehicle. Vibrations transferred to the cabin where passengers sit is to a certain extent influenced by tires. Plushness (or road isolation), nibble (steering wheel oscillations) or shake are factors [4] that relate to vehicle ride that are evaluated from a tire's standpoint.
3. Noise: Tread design, tread stiffness, its sequencing pattern and the tire construction influences the tire noise that is produced usually at high speeds. For purposes of analysis, tire noise is divided into air-borne noise and structure borne noise. A few techniques like tread element sequencing exist today in order to reduce tire noise.
4. Endurance: This is another important criterion involved in the design of tires. While the test procedure for evaluating it varies from organization to organization, it involves putting the tires through a large number of cycles at maximum load and inflation pressure conditions.

5. Wear: It is traditionally evaluated through outdoor tests where sets of tires are driven at prescribed speeds on a known course to evaluate wear rate. It is usually measured in terms of miles covered per millimeter of tread depth loss or as the tread depth loss per increment in mileage [4]. External conditions like environmental factors and road conditions, vehicle alignment, loads as well as acceleration and deceleration levels influence wear. Efforts are taken to standardize and minimize these, as controlling them is critical in the repeatability of these measurements. Irregular wear such as heel and toe, cupping, shoulder wear or gravel chip is also important and is responsible for shortening the tire's life.

1.5.1.2 Static Properties

1. **Contact Patch Dimensions:**

   When a tire is loaded with the weight of the vehicle, it gets flattened at the bottom near its contact with the road. This flattened portion is in complete contact with the road is defined as the contact patch of that tire. As it is loaded with more and more weight, the dimensions of this contact patch tend to increase, on account of the elasticity of the tire. At lower loads, this shape is usually an oval and then tends to become more rectangular with an increase in load. Dimensions of this contact patch are important as they determine the shear forces generated that are important from the point of view of the vehicle motion. Static contact patch dimensions can be measured, for example, by placing the loaded tire on a sheet of carbon paper and extracting the dimensions from the print. Figure 1.4 illustrates the contact patch shape [2]. Here, a_c and b_c are the half-lengths and breadths of the contact patch and c is the shape factor.

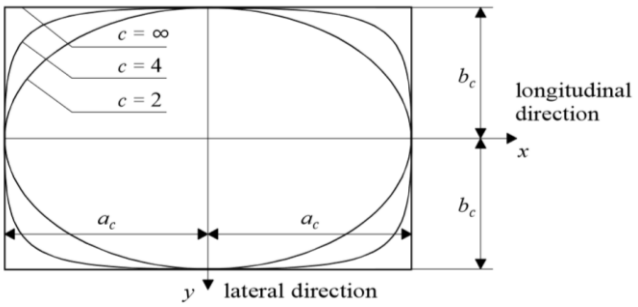

Figure 1.4: Contact Patch Dimensions [2]-
Peter W.A. Zegelaar, 'The dynamic response of tires to brake torque variations and road unevenness', Ph.D. thesis, Delft University of Technology, Netherlands, 1998. Used under fair use 2015.

2. **Vertical Tire Stiffness:**

The vertical load on the tire that causes a unit elastic deflection in the tire in the same direction can be defined as the vertical stiffness of that tire. This is an important characteristic for a number of reasons [3] such as: (i) The vertical tire stiffness influences the natural frequencies of the vertical vibrations of the tire. (ii) The tire is excited by the road unevenness through the vertical tire stiffness. A number of methods exist to measure the static stiffness of a tire [3]:

a. Static stiffness of a non-rotating tire can be obtained by measuring the settling value of the vertical force after increasing the deflection very slowly.
b. Dynamic stiffness of a rotating as well as non-rotating tire can be obtained from small amplitudes of random axle height vibrations around a number of vertical loads and velocities.
c. Dynamic stiffness of a rotating as well as non-rotating tire can also be obtained from large sinusoidal axle height motions at a number of velocities at low frequencies.

d. The vertical force obtained from a stationary rolling tire at various constant axle heights and velocities also give the Force vs. Deflection characteristics.

3. **Inertia Properties of the Tire:**

The mass and inertia of the tire has a large impact on the dynamic properties of the tire. Mass of the tire and rim can be measured directly. Moments of inertia about the wheel axis (y-axis) for both the rim as well as a combination of the tire and rim, can be measured indirectly by measuring the natural frequency of the wheel rotating about the wheel axis, constrained by a known additional rotational spring. The moment of inertia of the tire can be obtained as the difference between the two values. For the purpose of the application of the rigid ring tire model as will be discussed in the chapter on modeling, the tire is divided into five components: two beads, two sidewalls and one tread-band. The two beads are assumed to move together with the rim, the tread-band moves with the outer rigid ring. The masses of these components can be measured and moments of inertia can be calculated by assuming them to be simple homogenous shapes.

4. **Effective Rolling Radius:**

With the tire being an elastic entity, a number of definitions arise for its radius depending on the application that the radius is being used for. The simplest definition is that of the free rolling radius of the tire which is the radius of the tire when measured at its rated inflation pressure without it being loaded. This radius is represented as r_f and is seen in Figure 1.5. Similarly, the concept of effective rolling radius arises when the tire is in operation. It can be calculated from the velocities of the tire. For a freely rolling wheel, it is thus a ratio of the forward speed and its speed of revolution. In addition to the velocity,

effective rolling radius is also a function of the load acting on the tire. Figure 5 shows this effective rolling radius represented as r_e. Also seen in Figure 5 is r and is the radius of the tire in the loaded case as measured from the center of the tire to the ground at the contact patch.

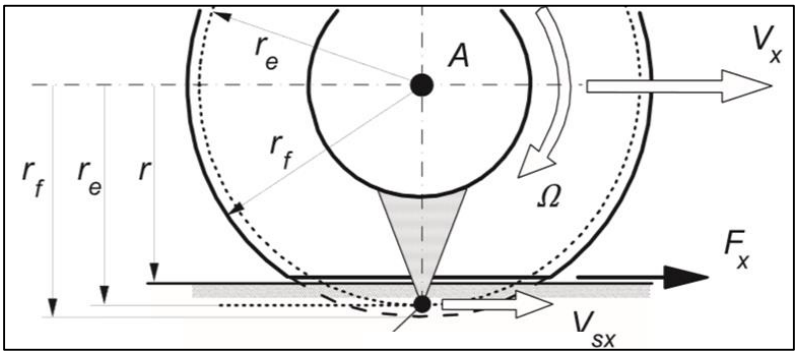

Figure 1.5: Effective Rolling Radius [5]-
Hans Pacejka, 'Tire and Vehicle Dynamics', Elsevier Ltd., 2012. Used under fair use 2015.

5. **Relaxation Length:**

   Relaxation length is an important parameter that governs the lag in the response of the tire to slip variations. It is the distance traveled equivalent of the time taken for a force to develop within the tire for step variations in tire slip. This is a transient phenomenon required for predicting fast events as occurring during antilock braking operations. A detailed formulation of this will be given in the section involving tire modeling.

6. **Rolling Resistance:**

   Rolling resistance as defined by Lindenmuth in [4] is the force necessary to overcome hysteretic losses in a rolling tire. This force can be measured by placing load cells in the wheel spindle and requires precise instrumentation, calibration, speed control and equipment alignment for repeatable results. This resistance is usually expressed as a coefficient- resistant force per 1000 units of load. This factor has the capacity to significantly influence the fuel

economy of the vehicle and depends on the inflation pressures maintained in operation. OE passenger car tires have rolling resistance coefficients that range from 0.007 to 0.01 when measured at thermal equilibrium. Rolling resistance is also a function of speed as will be seen in its formulation in the section on modeling.

7. **Tire Enveloping:**

   For any given road profile under consideration, it is seen that the road is never perfectly flat, no matter how smooth the road seems. This unevenness in the road profile is transferred to the tire in a complex way. The built-in flexibility in the geometry of the tire makes them act as geometric filters, smoothening the sharp edges as they transfer the unevenness in the direction of the load transfer. This property is known as the enveloping behavior of the tire and is illustrated in Figure 1.6. This property is modeled into the system using the Tandem Elliptical Cam Model as outlined in modeling.

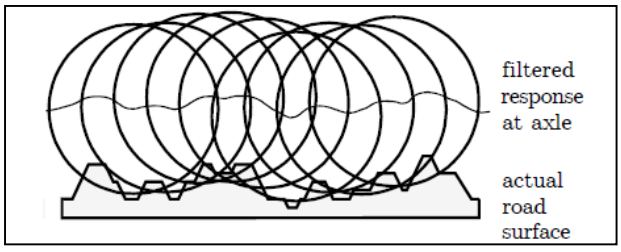

Figure 1.6: Tire Enveloping Property [2]-
Peter W.A. Zegelaar, 'The dynamic response of tires to brake torque variations and road unevenness', Ph.D. thesis, Delft University of Technology, Netherlands, 1998. Used under fair use 2015.

1.5.1.3 Tire Models

Modeling tires from the point of view of vehicle dynamics can be classified into those involving the fundamental laws on which the model is designed, and the application that they are designed for:

Empirical Models: These models are derived based on fitted experimental data. These models are useful from the point of view of their accuracy in predicting the force responses as their output is purely based on previously collected data. The magic formula by Pacejka [5] is the most famous empirical model that is used for vehicle dynamics analysis.

Physical Tire Models: These tire models are based on the analytical derivations using physical laws. Parameters are based on actual measurable entities and thus have a physical significance, as opposed to parameters from empirical models.

Depending on the application that the model is being used for, they can be classified into Steady State and Transient response models:

Steady State Response: A situation in which the variations in the input quantities to the tire such as vertical load, slip, etc. are low can be classified as steady state responses. Examples of such type of responses include slow steer turns and slow steer lane changes.

Transient Response: Vehicle dynamic maneuvers that involve rapid variations in slip with time can be classified as transient response maneuvers. During rapid variations, the forces in the tires are not generated instantaneously as explained in the section on relaxation length. Transient models account for the effects of relaxation length and predict force responses more accurately. Maneuvers like high speed double lane change classify as transient responses.

Further, tire models can also be classified based on the pavement that they are being modeled to travel on. Applications for highway grade roads like the rigid ring model [2] are significantly different from those involving off road soft soil as outlined by Taheri Sh. [6].

1.5.2 Antilock Braking Systems

The problem imposed by antilock braking is a highly nonlinear one due to the complicated relationship between friction and slip. Another factor in addition to this is that the linear velocity of the wheel cannot be measured directly. It has to be estimated. The friction between the road and the tire, too, is not readily measurable and requires complicated sensors. A number of control approaches have been employed in the past to tackle this problem as outlined by Aly et. al. in [7], and work mainly through control of two states: Wheel Slip and Wheel Acceleration.

Classical control has been used to analyze and improve the dynamic performance of the vehicle. As shown by [8], the PID controller proves to reduce the stopping distance of both the two- and four- wheel steer vehicles. Its simple design however has clear limitations of performance. It does not possess the robustness required for practical applications. However, a non-linear PID (NPID) controller algorithm, as developed by Jiang in [9], has a much more robust control and is easy to tune. The NPID controller has shorter stopping distance and has a better velocity performance than the loop-shaping and conventional PID controller. Optimal Control using Lyapunov based control laws guarantee bounded control action and can cope with input constraints. The closed loop system properties are such that they eliminate the friction estimator if the closed loop system is operating in the unstable region of the friction curve. Changes in road conditions imply continuous adaptation in controller

parameters. Wang, et al [10] compared the design process of back-stepping approach ABS through Multiple Model Adaptive Controllers (MMAC). The four models of high, medium, fixed and low adhesion were used within MMAC. Simulations on a quarter car vehicle using the MMAC proved to control wheel slip more accurately, have a higher robustness and therefore improve ABS performance effectively. Robust Control methods, like sliding mode control, is another important control methodology that has been investigated. A problem of concern associated with them is the lack of direct slip measurements. J.K. Hendrick et al. have suggested a modification of the technique known as slide mode control. This technique has proven to be robust to modeling errors and disturbance rejection capabilities. Adaptive control methods based on gain scheduling as presented by [11] shows capabilities of limiting wheel slip while tracking on a snow road, and has a satisfactory coordination between wheel torque and wheel steering. Intelligent control based on Fuzzy logic algorithms (FC) have been proposed to tackle the problem of unknown environmental parameters [12]. However the large amount of fuzzy rules make the analysis too complex. To tackle this problem fuzzy sliding model control (FSMC) design methods are proposed since they require only one variable to be defined as the fuzzy input variable and hence require fewer fuzzy rules as compared to FC [13].

1.5.3 Vehicles

An understanding of the vehicle behavior can usually be accomplished using two approaches: (1) Using empirical data or (2) using the analytical approach. The empirical method usually relies on trial and error that involves studying the vehicle performance to understand what factors affect it and in which way. This is not the

most reliable method of understanding vehicle performance and can often lead to incorrect or partially correct conclusions. For this reason, the analytical approach is preferred over the empirical approach. The analytical approach involves a mechanistic understanding of how changes in vehicle design change different performance parameters, as they are based on the laws of physics. Algebraic and differential equations can be used to relate the control parameters to the performance parameters of interest. This enables following an approach that involves reaching systematic parameter based targets.

A number of models exist which enable prediction of vehicle performance. The models can be made as complex as the level of detail and the degree of accuracy desired in the prediction of the parameters involved. A few of these simple models used for studying steady state vehicle behavior are explained here:

The two-degree of freedom bicycle model is the most simplified vehicle dynamics model. An illustration of this model is shown in Figure 1.7. The model represents the lateral and yaw motions associated with the vehicle. This highly simplified model finds applications when it is not desirable or necessary to study the motion in the longitudinal direction, as it does not affect the lateral or yaw stability of the vehicle.

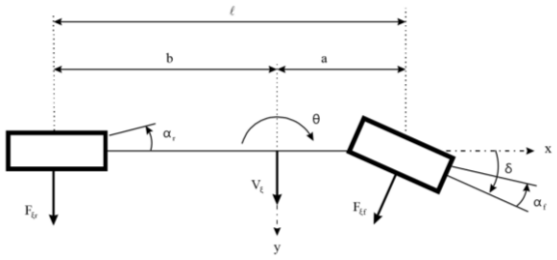

Figure 1.7: Two DOF Bicycle Model

A three-degree of freedom model can be considered next where the vehicle is considered to be moving on the same horizontal plane as shown in Figure 1.7, however is considered to have two displacements- one in the lateral direction, and the other in the longitudinal direction. The third degree of freedom represents the yaw motion of the vehicle. The path trajectory of a vehicle can be calculated using this model.

The two- and three- degree of freedom models as described above account for motion in a single horizontal plane. More realistic motions of the vehicle can be studied by adding motion of the vehicle in additional planes. A six-degree of freedom model can be studied with the help of a two track vehicle. For the six-degree of freedom model, in addition to the motions described earlier, it can also account for the vertical movement, the roll and the pitch motions of the vehicle. Figure 1.8 shows the representation of such a model as illustrated by, which can be used to analyze the motions described above.

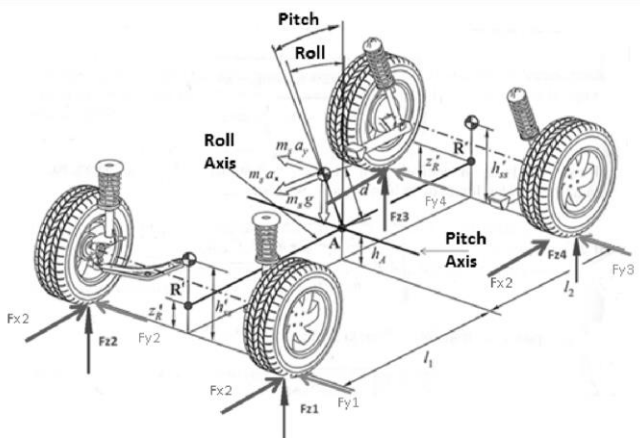

Figure 1.8: Six DOF Vehicle Model

For applications that involve a detailed study of the straight line motions of the vehicle, a vertical vehicle model with 7 degrees of motion is quite useful. This model does not involve lateral or yawing degrees of freedom on account of its motion in

the longitudinal direction. Instead, it consists of the vertical dynamics of the wheel as shown in Figure 1.9 as given by [14]. This model has 3 degrees of freedom for its vertical, roll and pitch motion, and 4 degrees of freedom at the 4 wheels to account for its vertical dynamics.

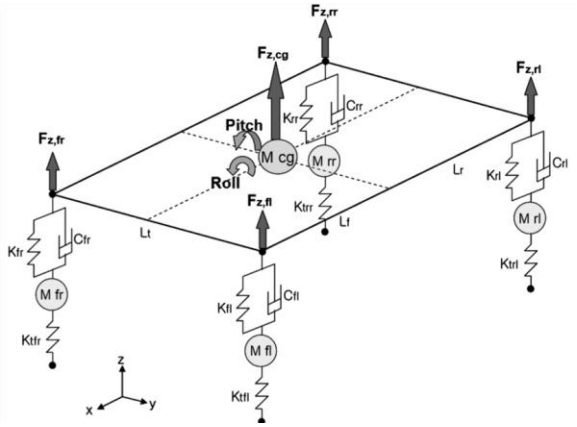

Figure 1.9: Seven DOF Vehicle Model [14]-
Jaehoon Lee, Jonghyun Lee, Seung-Jin, Heo, 'Full vehicle dynamic modeling for Chassis Control', FISITA, F2008-SC-021. Used under fair use 2015.

At times, it is imperative to study certain tire dynamics without the need of a complete vehicle model. A Quarter Car Model that employs a single wheel along with its suspension system is most suitable in such situations. It proves to be most useful for ride analysis as well as braking studies. It is a computationally inexpensive substitute for applications that do not involve dynamics of the complete vehicle. Figure 1.10 shows such a quarter car model as developed by Srikanth [3]

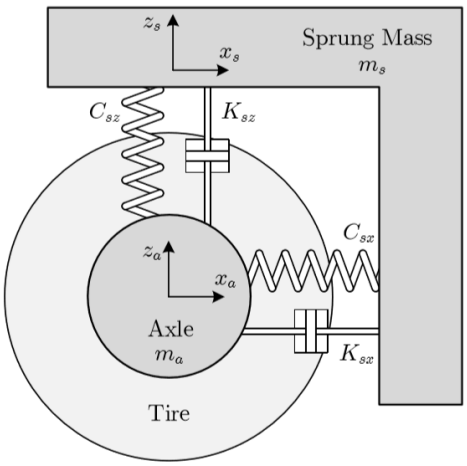

Figure 1.10: Quarter Car Model [3]-
Srikanth Sivaramakrishnan, 'Discrete Tire Modeling for Antilock Braking System Simulations', M.S. thesis, Virginia Tech, Blacksburg, VA, 2013. Used under fair use 2015.

Chapter 2:

System Modeling

2.1 Tire Model

2.1.1 Enveloping: Tandem Elliptical Cam Model

The Tandem Elliptical Cam Model developed by Schmeitz [15] is used to model the enveloping property of the tire as explained earlier. Figure 2.1 shows the diagrammatic interpretation of this semi-empirical model.

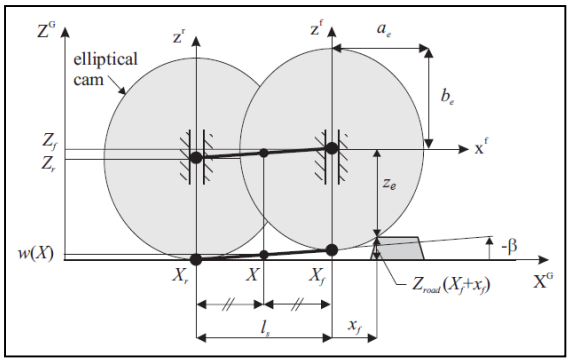

Figure 2.1: Tandem Elliptical Cam Model [15]-
A. Schmeitz, 'A Semi-Empirical Three-Dimensional Model of the Pneumatic Tyre Rolling over Arbitrarily Uneven Road Surfaces', Ph.D. thesis, Delft University of Technology, 2004. Used under fair use 2015.

The model consists of two elliptic shaped cams positioned in tandem connected by rods. The cams are constrained to move only in the vertical direction as they move over uneven road surfaces. This is represented in the figure by the rails shown around the center of these cams.

With this version of the Tandem Elliptical Cam Model designed for suiting an In-Plane tire model, it requires inputs of the x and z coordinates of the road. These co-ordinates are then transformed by the enveloping model into an effective height and slope for the base plane of the model as shown in the figure. The effective height of the inclined plane is calculated at its midpoint. The following is a guide to the abbreviations used in the formulas used in the model:

$w(X)$ - Effective Height of the bottom plane (m)

$\beta(X)$ - Slope of the bottom plane (deg)

Z_f - Global height of the front cam (m)

Z_r - Global height of the rear cam (m)

a_e - Height of the cam (m)

b_e - Width of the cam (m)

l_s - Cam separation (m)

x_f And z_f - Local position coordinates for the front ellipse

z_e - Vertical distance between local X-axis and ellipse (m)

The effective height is calculated as:

$$w(X) = \frac{Z_f + Z_r}{2} - b_e \tag{2.1}$$

The slope of the plane us calculating using:

$$\beta(X) = \arctan \frac{Z_r - Z_f}{l_s} \tag{2.2}$$

Equation for the ellipse in the local coordinate system can be given as:

$$\left(\frac{x_f}{a_e}\right)^{c_e} + \left(\frac{z_f}{b_e}\right)^{c_e} = 1 \tag{2.3}$$

z_e at a position x_f can be calculated using:

$$z_e(x_f) = \left| b_e \times \left(1 - \left(\frac{|x_f|}{a_e}\right)^{c_e}\right)^{\frac{1}{c_e}} \right| \tag{2.4}$$

Calculations for z_e enable calculations for the global height of the front ellipse Z_f using the maximal relation as the sum of the road height and the vertical distance between the ellipse contact point and the center using:

$$Z_f = \max[Z_{road}(X_f + x_f) + z_e(x_f)] \qquad \forall\ x_f \in [-a_e, a_e] \tag{2.5}$$

Cam separation l_s is a function of the vertical load on the tire and can be calculated based on the contact length $2a$ and a model parameter p_{ls} as:

$$l_s = p_{ls} \times 2a \tag{2.6}$$

2.1.2 Tire: Rigid Ring Model

For modeling the tire, the Rigid Ring Tire Model as explained by Zegelaar [2], has been adopted. The model assumes the tire belt to be a rigid ring connected to the axle through a series of springs and dampers which represent the pressurized side-

walls. A transient slip model serves as the contact model between the tire and the road. Figure 2.2 shows the Rigid Ring Tire Model.

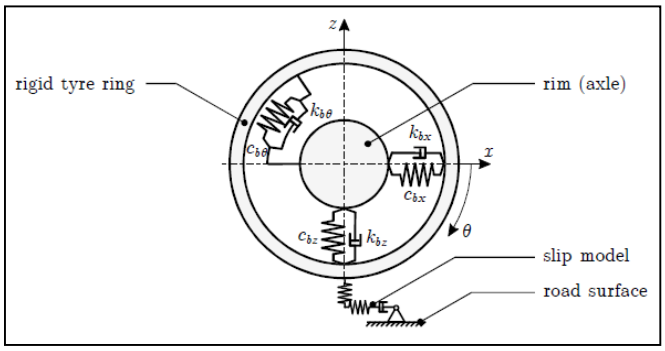

Figure 2.2: Rigid Ring Tire Model [2]-
Peter W.A. Zegelaar, 'The dynamic response of tires to brake torque variations and road unevenness', Ph.D. thesis, Delft University of Technology, Netherlands, 1998. Used under fair use 2015.

Figure 2.3 shows the mechanics of the deformations assumed to occur in this tire model. The wheel is assumed to be rotating at a uniform angular velocity of Ω and x_a and z_a represent the motions of the axle in the X and Z directions. A rotation of φ is assumed to take place in the ring resulting in the displacement of a point to the position O. The motion of the axle involving the translation by x_a and z_a and rotation by θ_a results in O being displaced to A. Post the displacement of the axle, the deflection of the sidewall results in point A moving to point B due to the rotation θ_b and a translation x_b and z_b in the X and Z directions of the rigid ring.

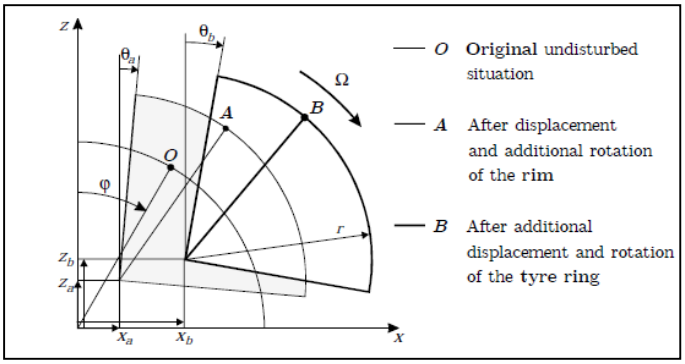

Figure 2.3: Deformations in Tire [2]-
Peter W.A. Zegelaar, 'The dynamic response of tires to brake torque variations and road unevenness', Ph.D. thesis, Delft University of Technology, Netherlands, 1998. Used under fair use 2015.

Equations of Motion:

The four-degrees of freedom of the rigid ring tire model of (1) Angular deflection of ring θ_a, (2) Horizontal deflection of the belt x_b, (3) Vertical deflection of the belt z_b and (4) Angular deflection of the axle θ_a. The equations of motion of this model are:

$$m_b\ddot{x}_b + k_{bx}(\dot{x}_b - \dot{x}_a) + c_{bx}(x_b - x_a) - k_{bz}(\Omega - \dot{\theta}_a)(z_b - z_a) = F_{cT}\cos\beta + F_{cN}\sin\beta \quad (2.7)$$

$$m_b\ddot{z}_b + k_{bz}(\dot{z}_b - \dot{z}_a) + c_{bz}(z_b - z_a) + k_{bx}(\Omega - \dot{\theta}_a)(x_b - x_a) = F_{cN}\cos\beta - F_{cT}\sin\beta \quad (2.8)$$

$$I_{by}\ddot{\theta}_b + k_{b\theta}(\dot{\theta}_b - \dot{\theta}_a) + c_{b\theta}(\theta_b - \theta_a) = -r_e F_{cT} + M_{cY} \quad (2.9)$$

$$I_{ay}\ddot{\theta}_a + k_{b\theta}(\dot{\theta}_a - \dot{\theta}_b) + c_{b\theta}(\theta_a - \theta_b) = M_{ay} \quad (2.10)$$

Forces at Axle:

Forces generated by the tire at the axle serve as outputs to the vehicle model and are calculated using:

$$F_{xt} = c_{bx}(x_b - x_a) + k_{bx}(\dot{x}_b - \dot{x}_a) - k_{bx}(\Omega + \dot{\theta}_a)(z_b - z_a) \tag{2.11}$$

$$F_{zt} = c_{bz}(z_b - z_a) + k_{bz}(\dot{z}_b - \dot{z}_a) + k_{bz}(\Omega + \dot{\theta}_a)(x_b - x_a) \tag{2.12}$$

Tire - Road Contact Model:

A contact model is important for the tread elements to simulate the transient slip. Tangential forces are generated due to slip ζ_{cx} that occurs in the contact patch. Variations in slip occur due to the dynamic interactions between the tread elements of the rolling tire and the ground. This contact is modeled using an analytical model as shown in the Figure 2.4 where the non-steady-state variations are modeled using first order approximations and based on the relaxation length and slip velocity calculations, as discussed ahead.

$$\sigma_c \times \dot{\zeta}_{cx} + |V_{cr}| = -V_{c,sx} \tag{2.13}$$

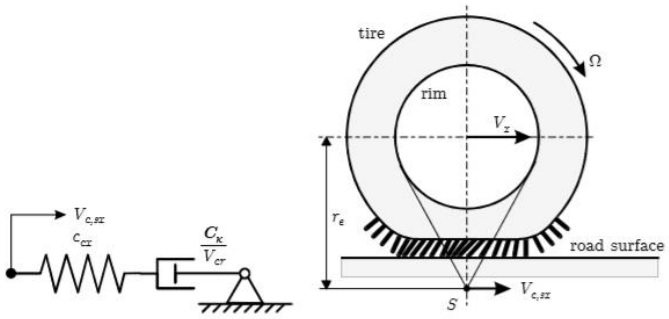

Figure 2.4: Tread Element Model & Brush Type Tread Elements [2]-
Peter W.A. Zegelaar, 'The dynamic response of tires to brake torque variations and road unevenness', Ph.D. thesis, Delft University of Technology, Netherlands, 1998. Used under fair use 2015.

Here, σ_c is the relaxation length of the contact patch. The linear rolling velocity of the belt V_{cr} is calculated using:

$$V_{cr} = r_e \times (\Omega + \dot{\theta}_b) \tag{2.14}$$

Slip Velocity:

The slip velocity of the belt is calculated as the difference between the linear velocity of the center of the ring along the road surface and its rolling velocity as shown in Equation 2.15. The influence of road disturbances on the effective rolling radius is accounted for within this equation.

$$V_{c,sx} = V_{cT} - V_{cr} = (\dot{x}_b \cos\beta - \dot{z}_b \sin\beta) - r_e(\Omega + \dot{\theta}_b) + \rho_z \frac{d\beta}{dt} \tag{2.15}$$

Relaxation Length:

The relaxation length can be calculated from local slip stiffness C_κ and the slip stiffness at free rolling $C_{\kappa 0}$:

$$\sigma_c = \sigma_{c0} \frac{C_\kappa}{C_{\kappa 0}} \tag{2.16}$$

Where, σ_{c0} is the relaxation length at free rolling and is half that of the contact length. The slip stiffness at free rolling $C_{\kappa 0}$ can be calculated from the unit tread element stiffness c_{px} and half the contact length a as:

$$C_{\kappa 0} = 2c_{px}a^2 \tag{2.17}$$

Equation 2.18 gives the local slip stiffness:

$$C_\kappa = \left(\frac{\partial F_x}{\partial \zeta} \right)_{\zeta = \zeta_{cx}} \tag{2.18}$$

Contact Patch:

Contact patch of the tire is a function of the load that acts on the tire. The area of this contact patch grows as the load on the tire increases. This non-linear relationship between the contact patch length and the normal load on it can be expressed using the following formula:

$$a = r_0\left(q_{ra2}\frac{F_{cN}}{C_z \cdot r_0} + q_{ra1}\sqrt{\frac{F_{cN}}{C_z \cdot r_0}} \right) \approx r_0\left(q_{ra2}\frac{\rho_0}{r_0} + q_{ra1}\sqrt{\frac{\rho_z}{r_0}} \right) \tag{2.19}$$

Where q_{ra1} and q_{ra2} are polynomial fit parameters that are obtained from experiments.

Sidewall Stiffness and Damping:

Due to symmetry, the stiffness and damping in the horizontal direction are assumed to be the same as those in the vertical direction and are represented by c_{bx} and k_{bx}. The rotational stiffness and damping are represented by $c_{b\theta}$ and $k_{b\theta}$. The stiffness and damping can be calculated from the natural frequencies of the in-plane rigid body modes of the unloaded, inflated tire that is mounted on a fixed spindle without contact with the ground as:

$$c_{bx0} = c_{bz0} = 4\pi^2 \times m_b \times f^2{}_{long} \tag{2.20}$$

$$c_{b\theta 0} = 4\pi^2 \times I_{by} \times f^2{}_{windup} \tag{2.21}$$

$$k_{bx0} = k_{bz0} = 4\pi \times \zeta_{long} \times m_b \times f_{long} \tag{2.22}$$

$$k_{b\theta 0} = 4\pi \times \zeta_{windup} \times I_{by} \times f_{windup} \tag{2.23}$$

Where, f_{long} is the primary eigen-frequency and ζ_{long} is the dimensionless damping factor of the longitudinal and vertical motion of the belt which is also known as the in-plane vertical mode.

Normal Force:

Represented by F_{cN}, the normal force is a product of the residual stiffness and the residual deflection in the contact patch. The normal force in the contact patch has a non-linear relation with the residual deflection and is represented as:

$$F_{cN} = \begin{cases} q_{Fzr3}\rho^3{}_{zr} + q_{Fzr2}\rho^2{}_{zr} + q_{Fzr1}\rho_{zr} & \text{if} \quad \rho_{zr} > 0 \\ 0 & \rho_{zr} \le 0 \end{cases} \tag{2.24}$$

Where q_{Fz1} and q_{Fz2} are the linear and quadratic factors in the total vertical load-deflection characteristics.

Tangential force:

The tangential forces are calculated form the brush model. The transient slip ζ_{cx} calculated from the slip model and the vertical load in the contact patch F_{cN} are used as inputs to the brush model. The brush model as shown in Figure 2.4 is a steady state physical tire model where the tread elements are assumed to behave like bristles with a stiffness c_{px} c per unit length of the tread. The force can be given by:

$$F_{cT} = \begin{cases} \mu F_{cN} \left\{ \left[3|\theta\zeta_{cx}| - 3|\theta\zeta_{cx}|^2 + |\theta\zeta_{cx}|^3 \right] \right\} \text{sgn}(\zeta_{cx}) & for |\zeta_{cx}| \le 1/\theta \\ \mu F_{cN} . \text{sgn}(\zeta_{cx}) & for |\zeta_{cx}| > 1/\theta \end{cases} \tag{2.25}$$

Where θ is the composite parameter.

Effective Rolling Radius:

The effective rolling radius as needed for calculations of slip velocity, can be calculated through an empirical relation using:

$$r_e = \Delta r - \frac{F_{z0}}{C_z}(D_{reff} \arctan(B_{reff} \frac{F_{cN}}{F_{z0}}) + F_{reff} \frac{F_{cN}}{F_{z0}}) \quad (2.26)$$

where B_{reff}, D_{reff} and F_{reff} are model parameters. Here, C_z is the total vertical stiffness.

Rolling Resistance:

Rolling resistance is accounted for in the equations of motion by assuming an external torque M_{cy}, acting on the ring. This torque can be given by:

$$M_{cy} = -r_e F_r F_{cN} \cdot \text{sgn}(\Omega + \dot{\theta}_b) \quad (2.27)$$

Where, r_e is the rolling resistance coefficient is assumed to be a non-linear function of speed.

2.2 Antilock Braking System Model

The antilock braking system model as designed by Ding [16] and used for the simulations consists of a pressure regulator module and a control algorithm. A number of standard assumptions were made in order to simplify the modeling process.

2.2.1 Pressure Regulation

The electromagnetic valves present in the Hydraulic Control Unit (HCU) are responsible for pressure regulation within the antilock braking system. Pressure is regulated using the three states: (1) Pressure increase, (2) Hold Pressure and (3) Pressure release.

Increase in pressure is assumed to be exponential and is calculated using the following relation:

$$P_w(t) = P_m - [(P_m - P_{w0})^{\phi_{inc}} - K_{inc}\phi_{inc}(t - t_0)]^{1/\phi_{inc}} \tag{2.28}$$

Where, P_{w0} is the wheel cylinder pressure at the previous time step

P_m is the pressure in the master cylinder.

$K_{inc} and \phi_{inc}$ are model parameters for the response characteristics of the brake system.

Pressure release in the brake cylinder is governed by the following expression:

$$P_w(t) = [(P_{w_0} - P_a)^{\phi_{dec}} - K_{dec}\phi_{dec}(t - t_0)]^{1/\phi_{inc}} + P_a \tag{2.29}$$

Where, P_a is the atmospheric pressure.

$K_{inc} and \phi_{inc}$ are selected based on the desired pressure decrease characteristics.

Pressure in the wheel cylinder is converted into brake torque M_{ay} using the relation:

$$M_{ay} = P_w \cdot C_P$$

where, C_P is the brake torque gain and assumes values based on the axle under consideration.

2.2.2 Brake States and Selection

A number of brake states are used in the braking control algorithm in order to achieve optimal control of slip and wheel acceleration:

Initialize: A proper build-up of pressure in the wheel cylinder before regulation is essential and this state ensures this by setting the pressure in the wheel cylinder to the pressure in the master cylinder.

Hold Brake pressure: Pressures in the wheel cylinder are held at the same value as that in the previous cycle when wheel slip and wheel accelerations fall in the desired range using this state.

Increase Brake Pressure: Brake pressures are increased from its current pressure up to the master cylinder pressure at a normal rate using this state.

Fast Increase Brake Pressure: Rough roads usually cause a change in the level of contact the tire maintains with the road. This change, tends to change the slip values of the tire drastically and require the pressure in the wheel cylinders to change at a rapid rate. Fast increase brake pressure is a state used in such circumstances.

Decrease Brake Pressure: This state is responsible for releasing the brake pressures from the wheel cylinders down to atmospheric pressure.

Step Increase Brake Pressure: This state is used to perform the two operations of increase brake pressure and hold brake pressure simultaneously. This state is mainly used when an increase in brake pressure is desired while maintaining the wheel accelerations without having to wait for the controller to perform its calculations.

Step Decrease Brake Pressure: This state operates on the same principle as described in Step Increase Brake Pressure while decreasing brake pressures.

Exit Braking: Reduction of the vehicle speed below a minimal threshold value causes this state to trigger as braking switches to manual mode.

A single controller is responsible for controlling the brake states on all the four wheels of the vehicle. Controller flags are responsible for controlling one wheel per cycle as the controlled wheel rotates after every cycle. The decision for state selection is made based on a set of rules and thresholds. Figure 2.5 shows the flowchart for control cycling whereas Figure 2.6 shows the flowchart for selection of brake states.

Model Assumptions

The following assumptions were made while modeling this antilock braking system for the sake of simplicity in modeling:

- The rate at which brake pressures are increased and decreased remain constant and cannot be changed while the simulation run is underway.
- Wheel slip and acceleration thresholds cannot be changed during the simulation.
- Valve delay is represented as a first order delay.
- Pressure in the brake line is considered to be proportional to the brake torque at the axle.
- Pressure in the master cylinder is assumed to be a constant value.
- Sensors are assumed to feed information regarding wheel slip and vehicle speed to the ABS controller.
- The time delay required to convert brake line pressure into brake torque is assumed to be constant.
- ABS is not activated below a minimal vehicle speed threshold.

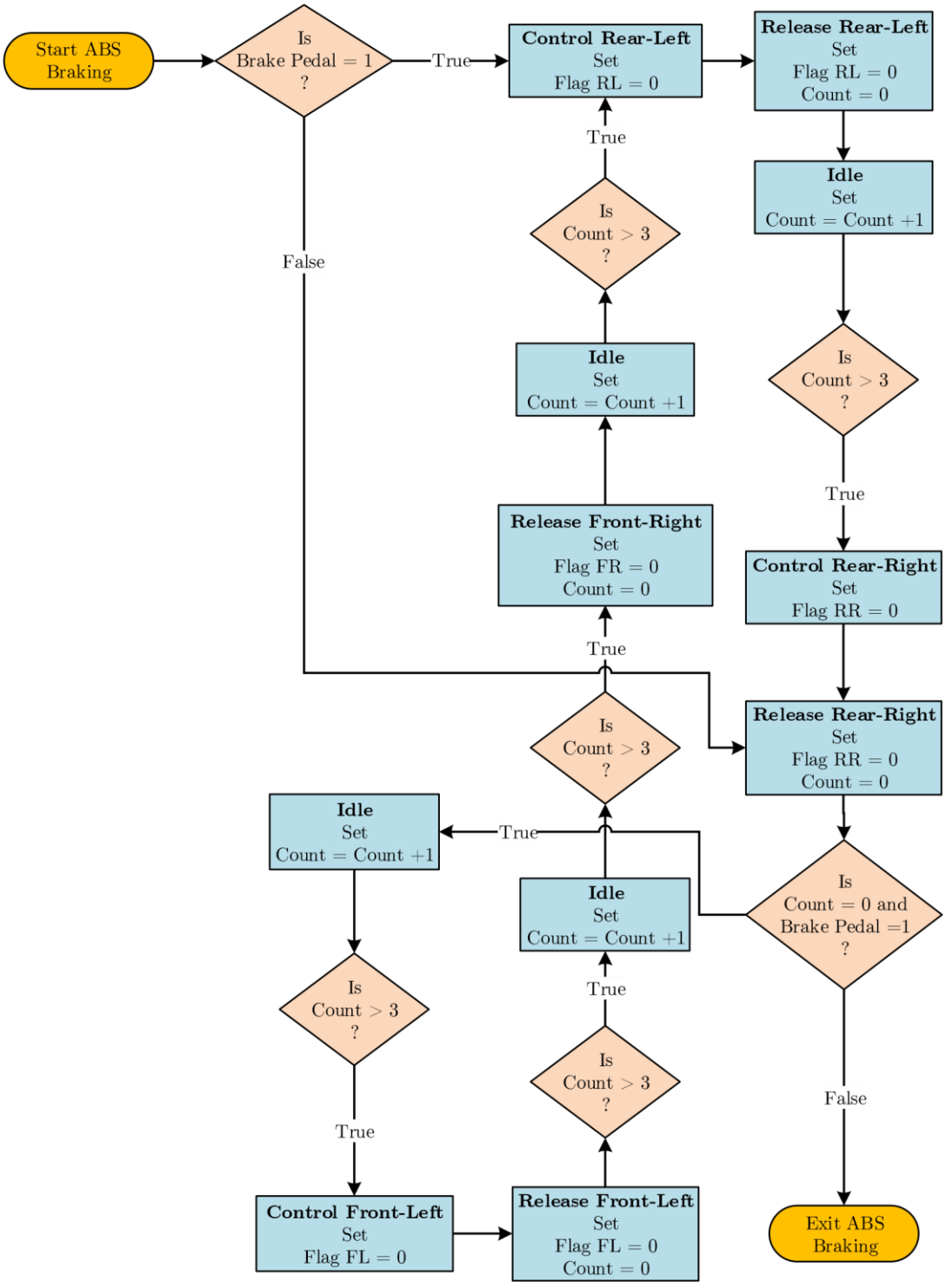

Figure 2.5: ABS Control Cycling between Different Tires

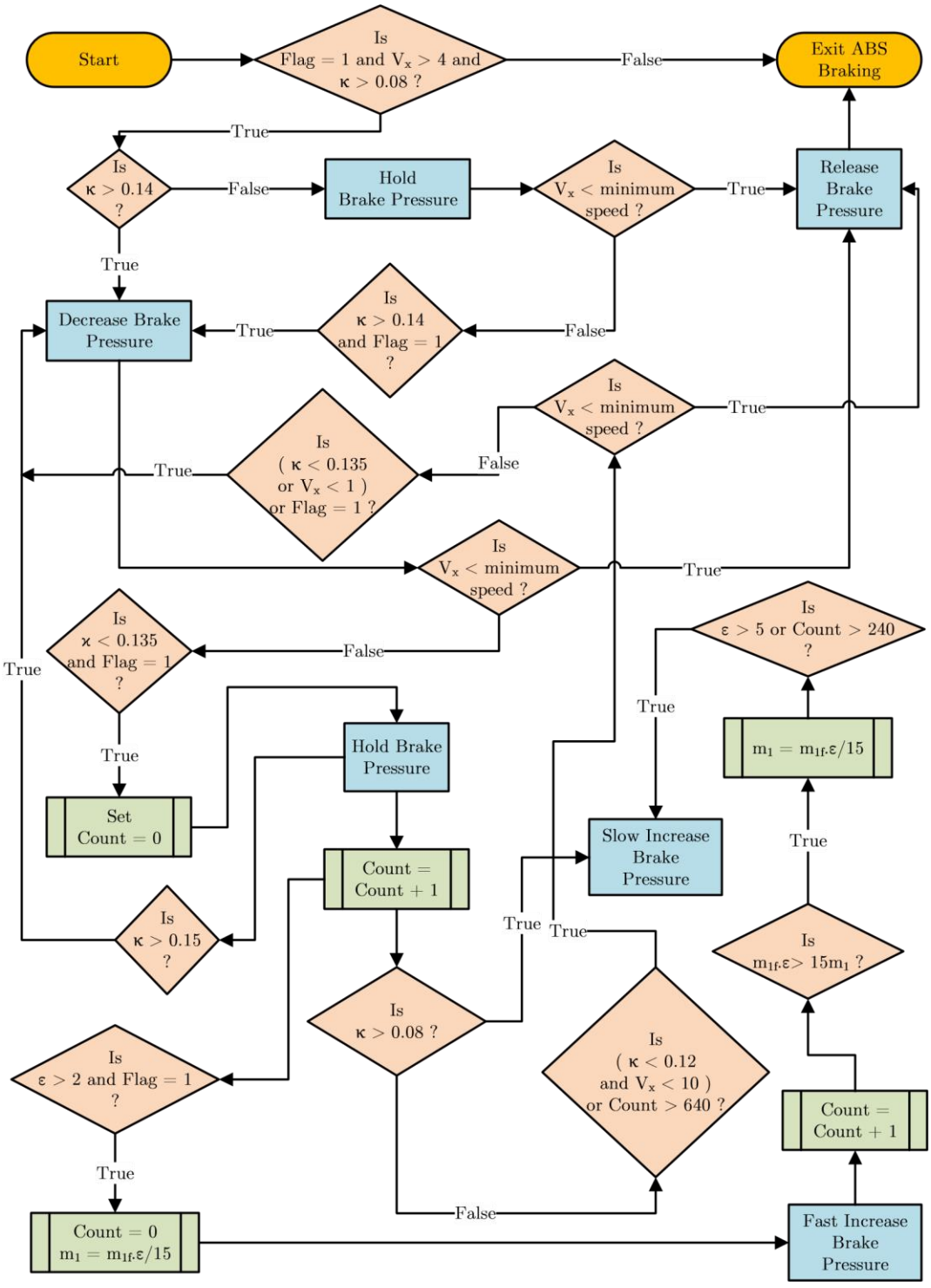

Figure 2.6: Selection of Brake States

2.3 Vehicle Model

The vehicle model was generated with the help of the commercially available software CarSim®. CarSim is a software package that predicts vehicle performance in response to driver controls such as acceleration, turning, braking, etc. for a vehicle being driven in a given environment as defined by the user. The math models used in CarSim® are capable of reproducing actual test results for various vehicle systems with a high level of accuracy. The models do not use information from the individual components as are assembled within the vehicle. For the same reason, fatigue, durability or high-frequency vibrations is not predicted using this software. The focus is more towards predicting vehicle behavior as it relates to vehicle handling. The models are generated using a symbolic multi-body code generator called VehicleSim Lisp which is highly optimized to achieve computations much faster than real-time during stand-alone use of the software.

In order to reproduce the behavior of a particular vehicle virtually, data from actual vehicle systems can be implemented in CarSim®. For the purpose of straight line braking simulations within the scope of the current work, suspension parameters, vehicle dimensions and weight details from an actual vehicle were implemented within CarSim®. For the sake of validation, the 2000 VW Jetta was used due to the availability of its data.

2.3.1 Suspension System

The suspension and steering systems can be implemented in CarSim® with the help of the data obtained from the Suspension Parameter Measurement Machine (SPMM). A suspension parameter measurement machine is responsible for measuring the kinematics and compliances (K&C) of a vehicle. Kinematics can be defined as the movement of the wheel due to the suspension displacements.

Whereas, compliances can be defined as the movement of the wheel due to road plane tire forces and usually arise from structural deflections of vehicle components and bushings.

Suspension parameters, in general are found through tests that involve isolating the different components in order to investigate specific parameters. K&C testing involves the vehicle being tested for different parameters like suspension spring stiffness, roll stiffness, etc. quasi-statically. In quasi-static testing, data is measured discretely between incremental displacements given to the suspension. The suspension system is given a certain amount of displacement, after which the procedure is stopped and the necessary vehicle and suspension forces and displacements are measured. While a particular suspension system is being tested, the lateral, longitudinal and vertical motion of the wheel center is measured in combination with change in steering angles, changes in camber angle and changes in caster angles [17]. Wheels of vehicles mounted on such suspension test rigs are usually supported on platforms known as ‘wheel pads’ or ‘wheel stations’, which replicate the road plane and are traditionally designed on air bearings. These air bearings allow the wheels to move freely without any resistance to lateral, longitudinal and steer movements during bounce tests, roll tests, etc. In addition, road plane forces and moments can also be applied to the wheel pads with the help of actuators. Forces in the longitudinal direction are capable of simulating braking, whereas forces in the lateral direction are capable of simulating vehicle cornering. Scale systems are designed into the wheel pads in order to measure the displacements that the wheels undergo as well as the forces that they are subjected to. At times when the center of pressure of the tire is desired, scale systems are built with multiple load cells, so that data from each of those load cells can be combined in order to find its cumulative center. During kinematics & compliance testing, it is highly important

to measure the position of wheel centers. These measurements are usually carried out with the help of either string potentiometers or other linear potentiometers and encoders. Figure 2.7 shows a diagram of the 'SPMM 5000' as produced by Anthony Best Dynamics, UK [18].

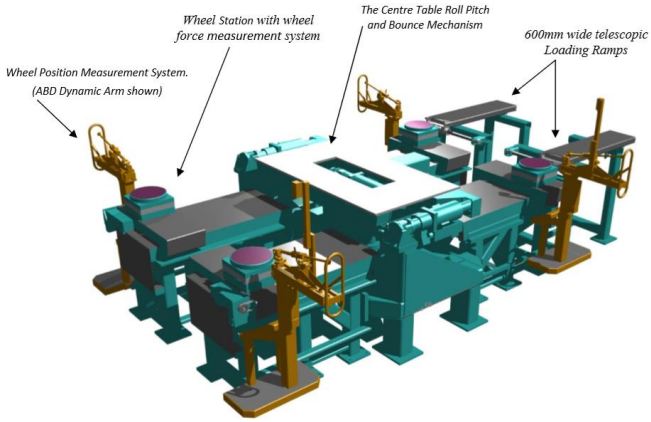

Figure 2.7: Suspension Parameter Measurement Machine [18]-
AB Dynamics, 'SPMM 5000, Outline Specification – SP20016 issue 2' available online at http://www.abd.uk.com/upload/files/2014-09-10_17-08-17_Sp20016%20i2%20SPMM%205000%20Outline%20Specification.pdf. Used under fair use 2015.

2.3.1.1 Implementation

The use of generic system-level parameters and non-linear tables for capturing vehicle behavior in CarSim® reduces the number of suspension models to just a few types, based on the fundamental kinematical behavior: Independent suspension, Solid Axle suspension and Twist beam suspension. The vehicle chosen for validation has an independent suspension in the front as well as rear. An independent suspension according to [19] can be defined as one in which vertical movement of one wheel does not cause noticeable movement of the other wheel if the anti-roll bar is disconnected. This means that the kinematical motions of each wheel are related only to the vertical deflection. In order to determine load transfer due to suspension

kinematical properties, lateral forces are transmitted to the sprung mass along the lines of action perpendicular to the path of constrained motion.

2.3.1.2 Jounce and Component Compression

The upward vertical displacement of the wheel center from some reference position on account of the suspension action is known as jounce. The movement is measured in the co-ordinate system of the sprung mass. Displacements in the opposite direction are referred to as rebound. The reference for zero jounce is taken with reference to the method used for K&C measurements.

- Wheel Center Height

  This is the vertical height of the wheel center as taken in the sprung mass co-ordinate system when the vehicle is loaded to its design load. Design load is considered as the weight of the sprung mass. Sprung mass can be defined in CarSim® in two ways. First, from the point of view of the vehicle weight on each wheel, center of gravity and un-sprung mass. The second is where they are defined only using sprung mass and inertia itself. Calculating initial wheel loads using static analysis becomes an indeterminate problem in this case due to friction, potential uneven ground and potential asymmetric features [19]. Due to this, CarSim makes certain assumptions to estimate these values, such as left/right or front/rear symmetry. This ambiguity vanishes as soon as simulation starts, as dynamic equations are able to solve for these loads. Data from the whole vehicle was implemented during modeling in order to avoid this ambiguity.
- Jounce at Design load

The reference position for jounce measurements can be defined either to be zero or a non-zero value. These values are used to apply offsets for suspension kinematics tables to obtain camber, toe, etc. Non-zero values effect in an adjustment to the vehicle ride height. This reference was set to zero to indicate that the vertical displacement was taken from the design position.

2.3.1.3 Stiffness Properties

- Ride Rates

  Ride rate includes stiffness that arises from the spring stiffness amplified with the mechanical ratio, as well as the stiffness that arises from the tires. Measurements of wheel rates, which are the change in force at the wheel center for a unit change in suspension compression can also be used directly to substitute spring rates amplified by the mechanical ratio, as is done for this model.

- Roll Stiffness

  Axle roll is resisted by the vertical suspension springs and by a torsional spring that accounts for the difference between the roll moment as predicted by the spring effects alone and the roll moment that is measured with the laboratory test rig. Although it is referred to as a torsional spring, the roll moment in the math model can be due to certain other factors such as bending of sheet metals, binding or twisting of linkages, etc. The roll moment defined in the model accounts for all the roll moment effects other than the main suspension springs.

2.3.1.4 Kinematics and Compliances

The following is a list of the kinematics and compliances that were implemented within CarSim.

Table 2.1: CarSim Implemented Parameters

Dimensional Details:		**Susp. Kinematics**		**Susp. Compliances**	
1	Wheel Base	1	Wheel Camber	1	Toe vs. Fx (deg/kN)
2	Track Width (L&R)	2	Wheel Toe	2	Steer vs. Fy (deg/kN)
3	Vehicle Height	3	X displacement vs Bounce	3	Steer vs. Mz (deg/N-m)
4	Vehicle Width	4	Camber Angle vs Bounce	4	Camber vs. Fx (deg/kN)
Weight Details:		5	Y displacement vs Bounce	5	Camber vs. Fy (deg/kN)
1	Front Left Wheel Reaction	6	Steer Angle vs Bounce	6	Inclination vs Mz(deg/kNm)
2	Front Right Wheel Reaction	7	Shock force vs Comp. Rate	7	Long Disp. vs. Fx (mm/N)
3	Rear Left Wheel Reaction	8	Dive Angle vs Bounce	8	Lateral Disp vs. Fy (mm/N)
4	Rear Right Wheel Reaction	9	Jounce at design load	9	Aux roll damp (Nmsec/deg)

2.4 Road Profiles

2.4.1 Data measurement

Although road profiling has been around for a long time, early efforts towards high-speed road profiling began in the 1960s with the introduction of the inertial

profilometers by General Motors. With a substantial knowledge of profiler design and technology existing in the industry, a number of proven methods for analyzing and interpreting data generated from them are currently available [20].

A road profile can be understood as a two-dimensional slice of a road, taken along an imaginary line. Profiles that are taken along the lateral direction of the road show super-elevations, crowns, rutting and other distress in the road designs. Profiles taken in the longitudinal direction show the design grade, roughness and texture of the road. Figure 2.8 shows an illustration of the road profiles taken in both the directions.

Road profilers are instruments used to produce a series of numbers related in a well-defined way to a true profile. A road profiler works by combining the following three measurements: (1) Reference elevation (2) Height relative to the reference and (3) longitudinal distance. A representation of such measurements is shown in Figure 2.9 [20].

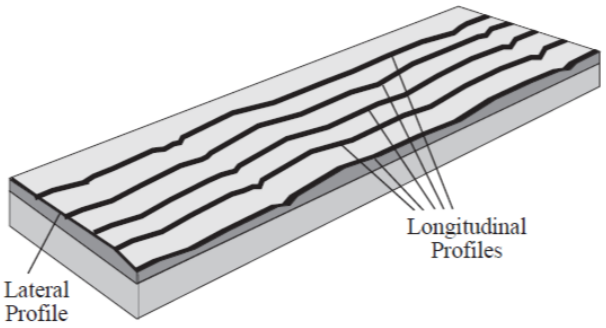

Figure 2.8: Road Profile Description [20]-
Michael W. Sayers, Steven M. Karamihas, 'The Little Book of Profiling', The Regent of the University of Michigan, September 1998. Used under fair use 2015.

The more advanced form of these measurements are carried out these days using Inertial Profilers, where an inertial reference is provided using accelerometers. Data processing algorithms are used to convert vertical accelerations obtained from these accelerometers to an inertial reference that defines the instantaneous height of the accelerometer within the vehicle which it is mounted. This way the height relative to the reference is that distance between the ground and the instantaneous position of the accelerometer. A non-contact laser transducer is used to perform these measurements. Longitudinal distances are calculated from an accurate measure of the speed of the vehicle.

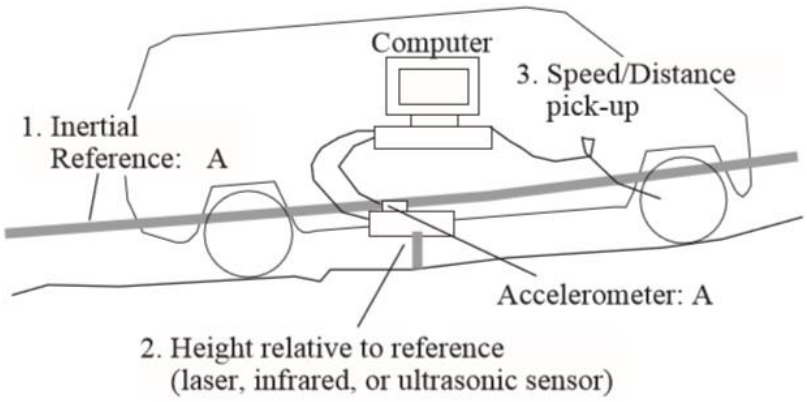

Figure 2.9: Profile Measurements [20]-
Michael W. Sayers, Steven M. Karamihas, 'The Little Book of Profiling', The Regent of the University of Michigan, September 1998. Used under fair use 2015.

2.4.2 Road Profiles

For the sake of simulations and in order to study the response of the vehicle in a wide variety of road cases, a number of road profiles were obtained and are explained below:

Smooth Asphalt Road: This is a road profile obtained form an asphalt concrete on a bound base. Data for this profile was obtained from the Long Term Pavement Performance (LTPP) database for a highway in the state of Oklahoma. It has the lowest level of disturbance. Measurement intervals for these measurements are longer at 150mm.

Joint Pavement Concrete Road: Data for this profile is also obtained from the LTPP database and has measurement intervals of 150mm. This data too comes from a highway in the state of Oklahoma but has sharper disturbances as compared to Smooth Asphalt road. This road is still classified as a smooth road despite the disturbances.

ISO Grade D Poor Asphalt: This road profile has short wavelength disturbances and was obtained from the Center for Tire Research (CenTiRe) to study braking performances on bad quality roads.

VTTI Smart Road: This road profile was measured at the Smart Road Facility at the Virginia Tech Transportation Institute (VTTI) and was also the road on which validation tests were performed for this model. Data from this road was processed in order to eliminate the gradient of the road. The detailed profile however, was used as it was.

Figures 2.10 and 2.11 show the profiles that have been discussed above and used for simulation.

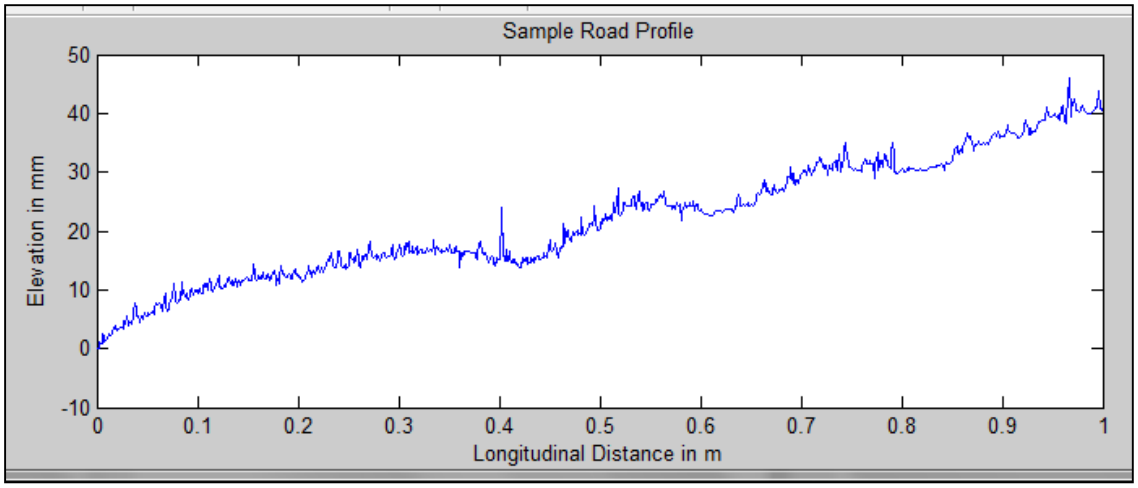

Figure 2.10: VTTI Road Profile

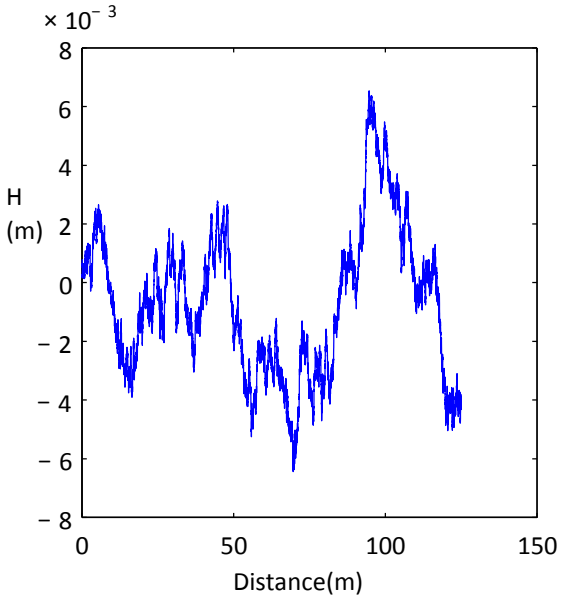

(a) Smooth Asphalt Road

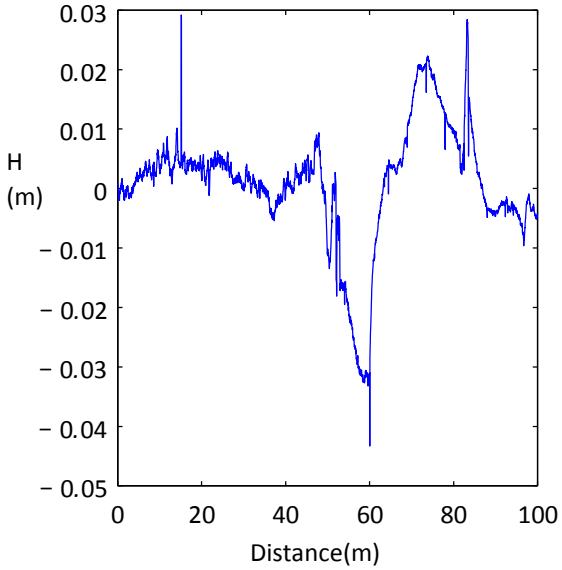

(b)Jointed Concrete

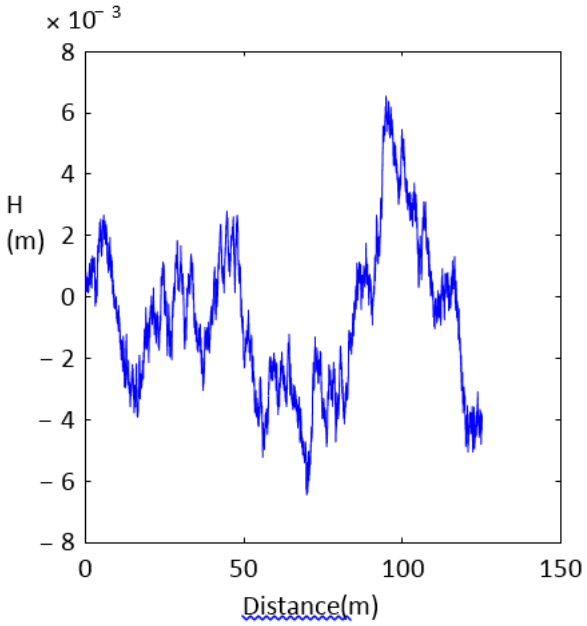

(c)ISO Grade D bad asphalt

Figure 2.11: Other Road Profiles

Chapter 3:

Simulation Tool

3.1 Parameter Exchange

3.1.1 Model Inputs and Outputs

Having established the models as described in Chapter 2, the next step in the process was to integrate the models together to form a simulation tool that is capable of predicting the straight line ABS performance accurately. Thus a simulation tool was created, where the outputs from one model served as the inputs to the other, as has been summarized in the Table 3.1:

Table 3.1: Model Input-Outputs

	Inputs		**Outputs**	
Model	**Parameters**	**Obtained from:**	**Parameters**	**Used for:**
Enveloping Model	Road Profile	External Input	Effective Height and slope of bottom plane	Tire Model
	Longitudinal Coordinate	Vehicle Model		
	Contact Patch Length	Tire Model		

Tire Model	Axle Motions & Axle Velocities	Vehicle Model	Longitudinal Slip	ABS Model
	Effective Height and slope of bottom plane	Enveloping Model	Longitudinal and Vertical Forces	Vehicle Model
	Brake Torques	ABS Model	Contact Patch Length	Enveloping Model
ABS Model	Vehicle Speed	Vehicle Model	Brake Torques	Tire Model
	Longitudinal Slip	Tire Model		
	Pedal Actuation	External Input		
Vehicle Model	Longitudinal and Vertical Forces	Tire Model	Axle Motions & Axle Velocities	Tire Model
			Vehicle Velocity	ABS Model

3.1.2 External Model Inputs

With the sheer number of inputs required for each of the models involved, automated parameter reading can be employed to avoid typing in individual parameter values for the tire and vehicle models.

All model constants for the tire parameters can be extracted from tire parameter (.tir) files. Further, data for the vehicle models can be imported into CarSim using parsfiles. Parsfiles are simple text files that can be used to feed parameters into all screens of CarSim all at once through file import. Data generated from K&C machines usually have the option of extracting parsfiles that can then be imported into CarSim for ready use by the Vehicle Sim solvers.

3.2 Simulink- CarSim Integration

Variable Import-Export

Vehicle Sim (VS), the main executable program of CarSim® supports extension of models using other software, options for which can be set through its model libraries. With the tire and vehicle models being designed in Simulink, the model libraries in CarSim® were set-up to communicate with the .mdl files in Simulink. Once the VS Solver is combined with Simulink, the vehicle model appears in the Simulink model as an external S-Function. For a particular setting of vehicle properties and test conditions within CarSim®, there exists a specific VS Solver that matches with its configuration. For a simulation run on a Windows OS PC, these VS Solvers are in the form of dynamically loaded library (DLL) files [21]. Simulink uses the VS solver files, when the VS browser is made to communicate with Simulink. A wrapper program, which is in the form of another DLL file is used for interfacing Simulink and the VS Solver. There is a close communication between the wrapper and the specific VS solver DLL during the run. When the VS solver is run from the VS browser, a simulation control file also called as ‘simfile’ is created in the folder containing the Simulink file. This file contains the path name for the VS solver, allowing the browser or a wrapper program to load and initiate the solver.

The import / export variables for the vehicle model as described in section 3.1 are defined within CarSim® in the Import/ Exports section. The variables available for import are described in a Readme file contained in CarSim® Program solvers which can also be viewed using a spreadsheet. After selecting the necessary parameters for import, they were selected to replace the same parameters that are solved by the models within CarSim®. The order of the import / export parameters were maintained consistent with that defined in the Simulink model. Initial values for the same were set to be consistent with those in Simulink.

Echo and End files:

When a VS solver runs, it creates summary files that list every parameter used. An _echo.par file is created before each run, and an _end.par file is created at the end of each run. As indicated by the PAR extension, the echo and end files follow the parsfile format. The echo file might also contain the initial conditions for the state variables in the simulation. In such cases, the file is sufficient to repeat the run in the exact same manner. End files are similar, except that they contain final values instead of initial values. Information in this file can be used to continue a run.

Log Files

Each run that is made in CarSim also has a corresponding log file that is created in text format. During initialization, it can echo every line that begins with the keyword LOG_ENTRY. It also logs every parsfile that is referenced with specific keywords. It logs the end of the run at termination. It can also log the processing of any triggered events during the run. Log files are useful from the point of view of debugging new externally created codes.

Simulation Procedure:

The simulation is started by specifying an initial speed for the vehicle in CarSim. The simulation is started at the speed of 18.05 m/s (~ 40mi/h). Antilock braking is initiated shortly after, and the simulation is stopped when the velocity of the vehicle reaches 2m/s in order to eliminate the effects of vehicle rock back when the motion stops. A driver path follower is employed in CarSim which is capable of keeping the vehicle on the specified path using closed loop controllers. For the current case of straight line ABS simulations, a straight line road path geometry is defined within CarSim that the controller follows.

Animations

CarSim® provides an option for viewing animations from a virtual camcorder that operates in a simulated 3D world. It does so by reading files with shape information of the vehicle and environment, motion information from the vehicle model, etc. The main advantage of these animations is to provide a quick visual on the behavior of the vehicle which instead could take time to analyze from the data plots. It also provides the option of overlaying animations, which is useful from the point of view of comparing vehicle behavior of two test cases.

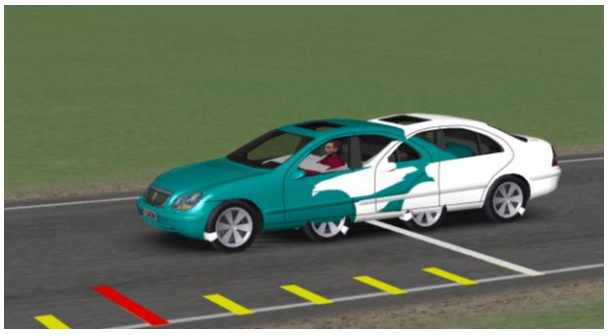

Figure 3.1: CarSim Overlay Animation for Comparisons

3.3 Vehicle Sim (VS) Based Programming

As the tire model is designed in Matlab/Simulink and the vehicle model is created in CarSim, it is important to ensure that the co-ordinate references taken for both are consistent with each other. There are differences in the original convention as followed in both, and Vehicle Sim based programming was used in CarSim to transform these co-ordinate references.

Rear Axle x-co-ordinate: Axle motions and axle velocities are imported from CarSim into the tire model as inputs. For the case of axle motions, CarSim considers the front axle center at the first time step to be the global x-coordinate for the vehicle. This naturally gives the rear axle a negative co-ordinate for the initial time steps until it passes the location where the front axle was at the first time step. To avoid numerical errors due to the negative coordinates, new parameters were defined for the rear axle within CarSim using VS based programming. The new parameters use the x-coordinate from the prior frame of reference and adds a distance equal to the vehicle wheel-base to its value. This way the x-co-ordinates are ensured to begin from 0 at the first time step for both the axles. Following shows the syntax used as accepted in VS programming.

```
DEFINE_OUTPUT XLR = X_L2 + LX_AXLE(2); units = m;
EXP_XLR;
```

Axle z-coordinates: CarSim considers the z coordinates of the axle imported in the tire model to have the axes origin at the center of contact patch. On the other hand, the tire model considers the axes origin to be where the axle is located at the first time step without the effect of static deflection. Considering the effect of static deflection due to the vehicle weight, the actual z-coordinate of the axle at the first time step becomes equal to that deflection in the negative direction. In order to

account for this difference statically and dynamically, the rolling radius of the tire as well as the static deflection is defined within CarSim. Static deflection is calculated by specifying the tire stiffness within CarSim. A syntax and notation similar to the above example is used to compensate for the difference in z-coordinates. EXP_*name*, as shown above is used to export the variable to the list of output variables in order to send it to Simulink.

3.4 Model Solving

3.4.1 Integration

A VS solver performs a run by performing calculations at closely spaced intervals of time, using the mathematical equations defined within CarSim®. Many of the state variables in a VS model are defined by a set of ordinary differential equations (ODEs) and are calculated using numerical integration of the derivatives of the state variables. CarSim recommends Adams Moulton second order integration method to solve for the Math Models which apply to the simulation used here. A math model time step of 0.0005secs (2000Hz) and an output file time step of 0.01secs (100Hz) is used in CarSim. A lower frequency is used for the output file in CarSim® in order to reduce the plotting time within CarSim®. When the variables are plotted from Simulink, they use the data from the math model with the higher frequency.

For Simulink, the fixed step solver has been identified as the best suited solver instead of variable step solvers as the specified frequency is matched with that specified in CarSim throughout the simulations. In addition, the error tolerances are kept at a low constant value throughout the simulation using the fixed solver. Further, the model parameters have continuous states, for which the continuous solver ODE3 (Bogocki Shampine) has been selected instead of a discrete solver. Finally, for the fixed step continuous solver, a frequency of 4000 Hz (i.e. time step of 0.00025sec)

which is half of the one in CarSim. This is a recommended practice when working with high frequency simulations like the current one for ABS as the two models communicate at every possible instance.

3.4.2 Algebraic Looping

Algebraic loops occur in Simulink models when a signal exists with only direct feedthrough blocks within the loop. 'Direct feedthrough' means that the block output depends on the value of an input port; the value of the input directly controls the value of the output. Algebraic loops usually occur when modeling physical systems due to conservation laws, or when a particular coordinate system is chosen for a model.

The nature of the tire-ABS model within Simulink is such that it has a tendency of generating algebraic loops. The resulting effect at times is that the solvers are not able to solve the loops and results in the simulation being stopped. It can also lead to excessively slow simulations, as the solvers try to solve the algebraic loops.

Iterative loops are used within Simulink to solve the algebraic loops. In addition, steps were taken to eliminate the loops altogether by specifying sufficient initial conditions as necessary as well as unit delay blocks as in the case of vehicle axle motion and velocity imports.

Simulation Tool:

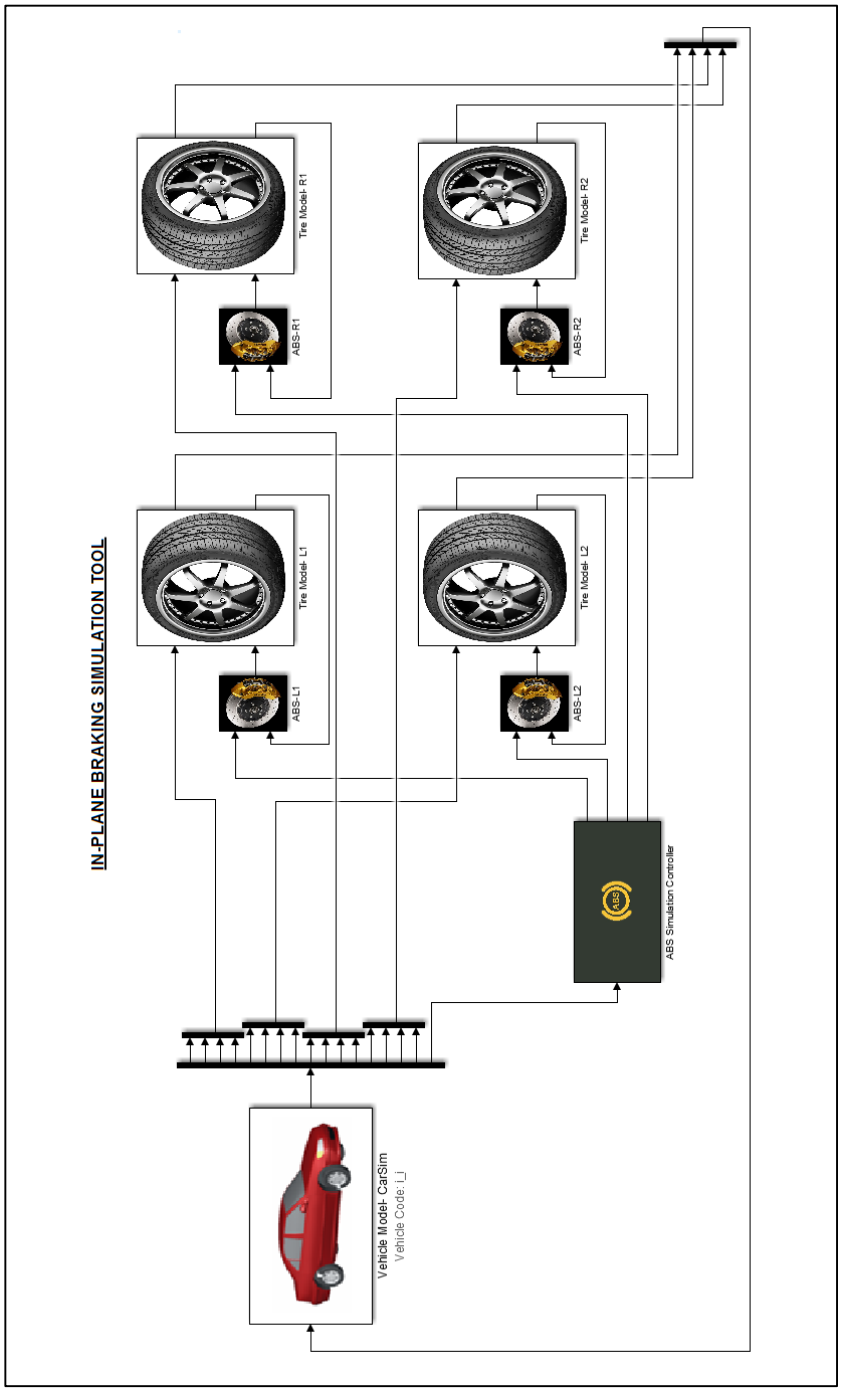

Figure 3.2: In-Plane Simulation Tool

Chapter 4:

Results and Validation

4.1 Simulation Results

The simulation results were plotted for the following parameters:

1. Vehicle and Wheel Velocities as shown in Figure 4.1
2. Braking Forces as shown in Figure 4.2
3. Braking Torques as shown in Figure 4.3
4. Longitudinal Slip Ratios as shown in Figure 4.4
5. Longitudinal Slip Ratio vs. Braking Forces as shown in Figure 4.5
6. Braking distances as shown in Figure 4.6

4.1.1 Discussions

The following pages show the result plots that were obtained for the jointed concrete pavement. Braking was activated at 2 seconds in the simulation to account for the settling of the states. A coefficient of friction of 0.9 was considered for this case. The following observations were made from the simulation results that were obtained.

1. Plots for the vehicle velocity (Figure 4.1) show a starting speed of 18.05 m/s. The simulation is cut off at 2m/s prior to the vehicle coming to a complete stop as was defined in the procedure. The velocity of the vehicle is seen to be slowing down almost linearly with respect to time. Wheel velocities are seen to be fluctuating for all the wheels indicating the ABS in action. The fall in the wheel velocities indicates a wheel lock tending to occur. The immediate

rise in the plot after the fall indicates release of brake pressure through ABS action. The front wheels are seen to be locking more number of times as compared to the rear wheels.

2. Plots for the longitudinal braking forces are seen to fluctuate rapidly on all four wheels on account of the changing brake torques on each wheel. Forces in the front are much higher as compared to the forces in the rear. This is seen because the vehicle has a configuration of being front heavy with an approximate weight distribution of 60%F/40%R. Further, the weight transfer to the front wheels on account of braking increases the braking requirement on the front wheels. Each spike in the braking force can be correlated to the spike in the wheel velocity on the same wheel.
3. The plots for brake torques clearly show the various brake states assumed by the controller like: increase brake pressure, decrease brake pressure, step increase brake pressure, hold, etc. The brake torque values in the front (900 Nm – 1800 Nm) are much more as compared to the rear (400 Nm – 1000 Nm) the same way braking forces are higher in the front as compared to the rear.
4. Plots for longitudinal slip ratio are analogous to wheel velocity plots and show that the front locks more times than the rear. Front slip values are also slightly higher as compared to the rear.
5. Plots for longitudinal slip ratio plotted against braking force show the effectiveness of the ABS algorithm of cycling the slip ratios around the peak region.
6. Figure 4.6 shows a comparison of the braking distances as obtained for the different road profiles used for the simulations. The braking distance for smooth asphalt was observed to be 20.95m, whereas the braking distance for jointed concrete was observed to be 20.87m and that for ISO grade D was observed to be 20.85m.

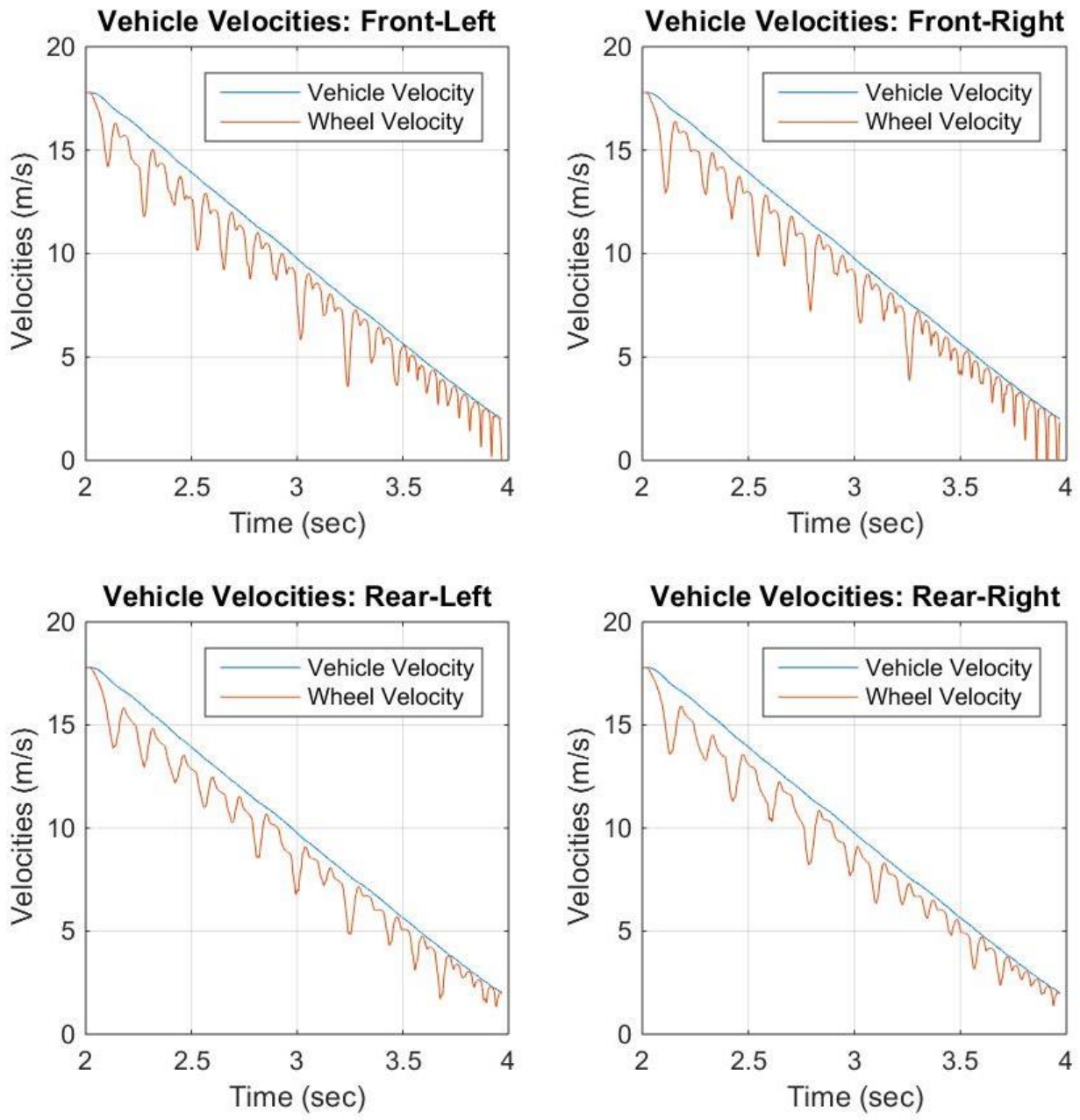

Figure 4.1: Simulation Results: Vehicle and Wheel Velocities

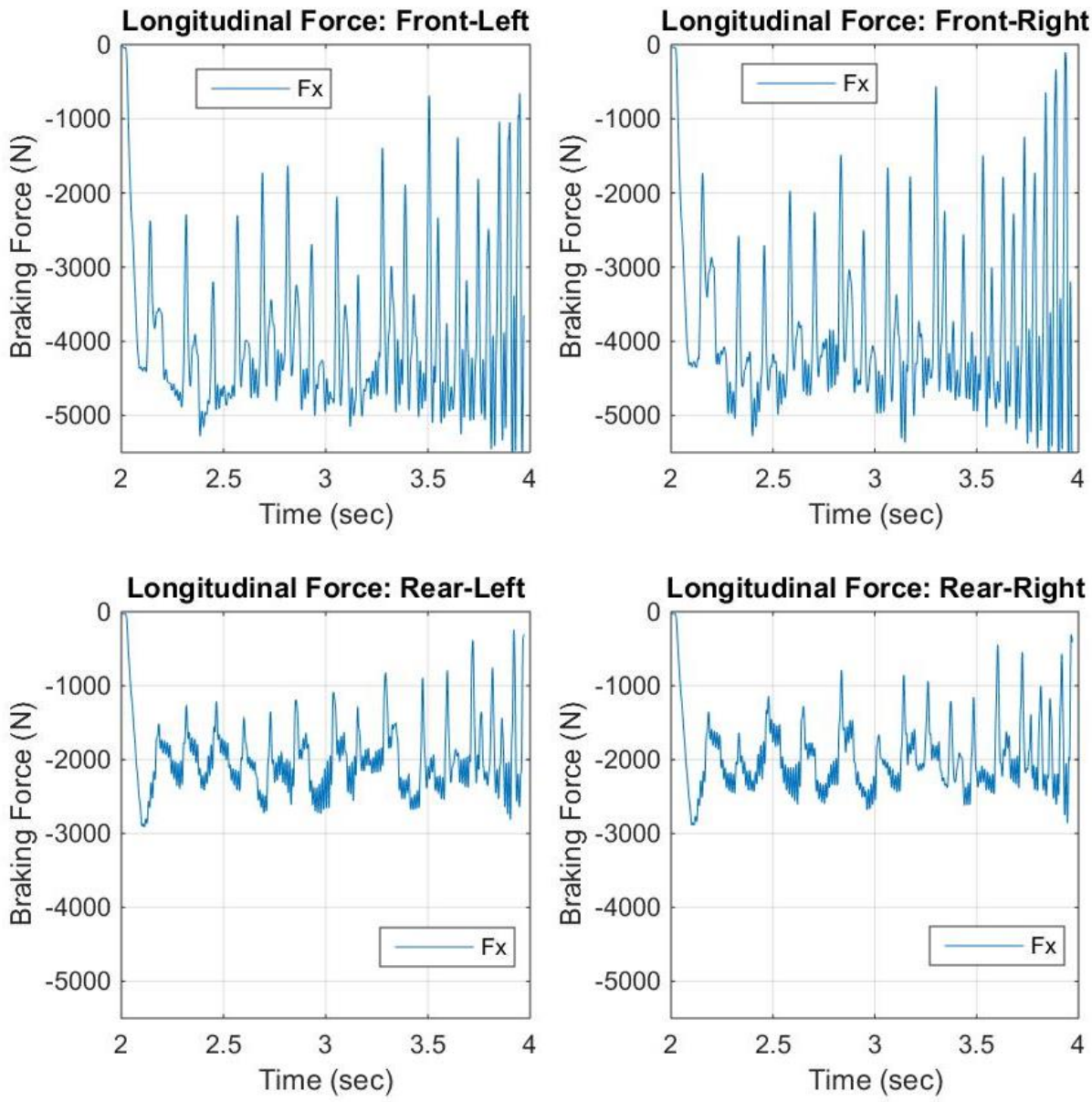

Figure 4.2: Simulation Results: Braking Forces

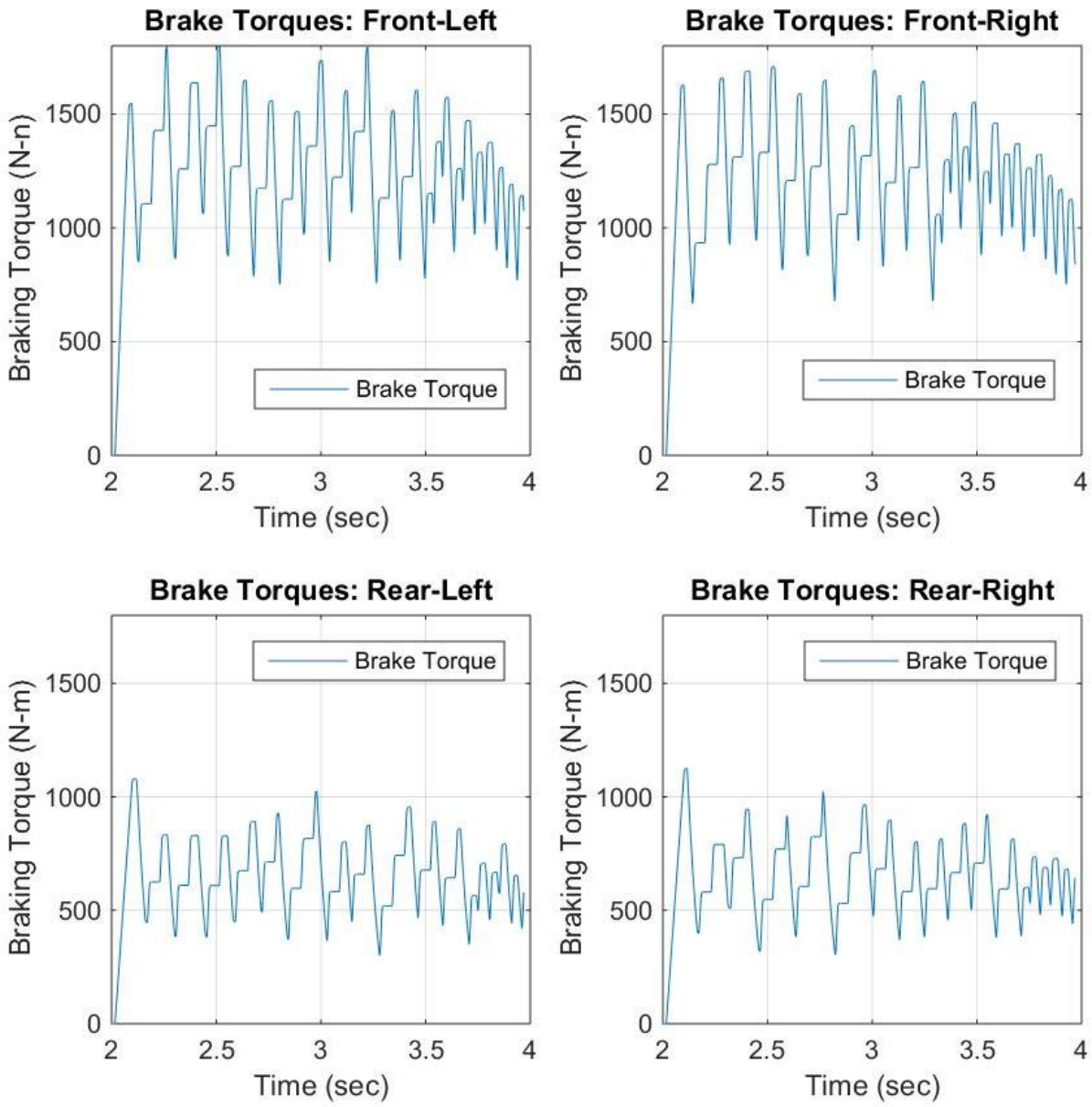

Figure 4.3: Simulation Results: Braking Torques

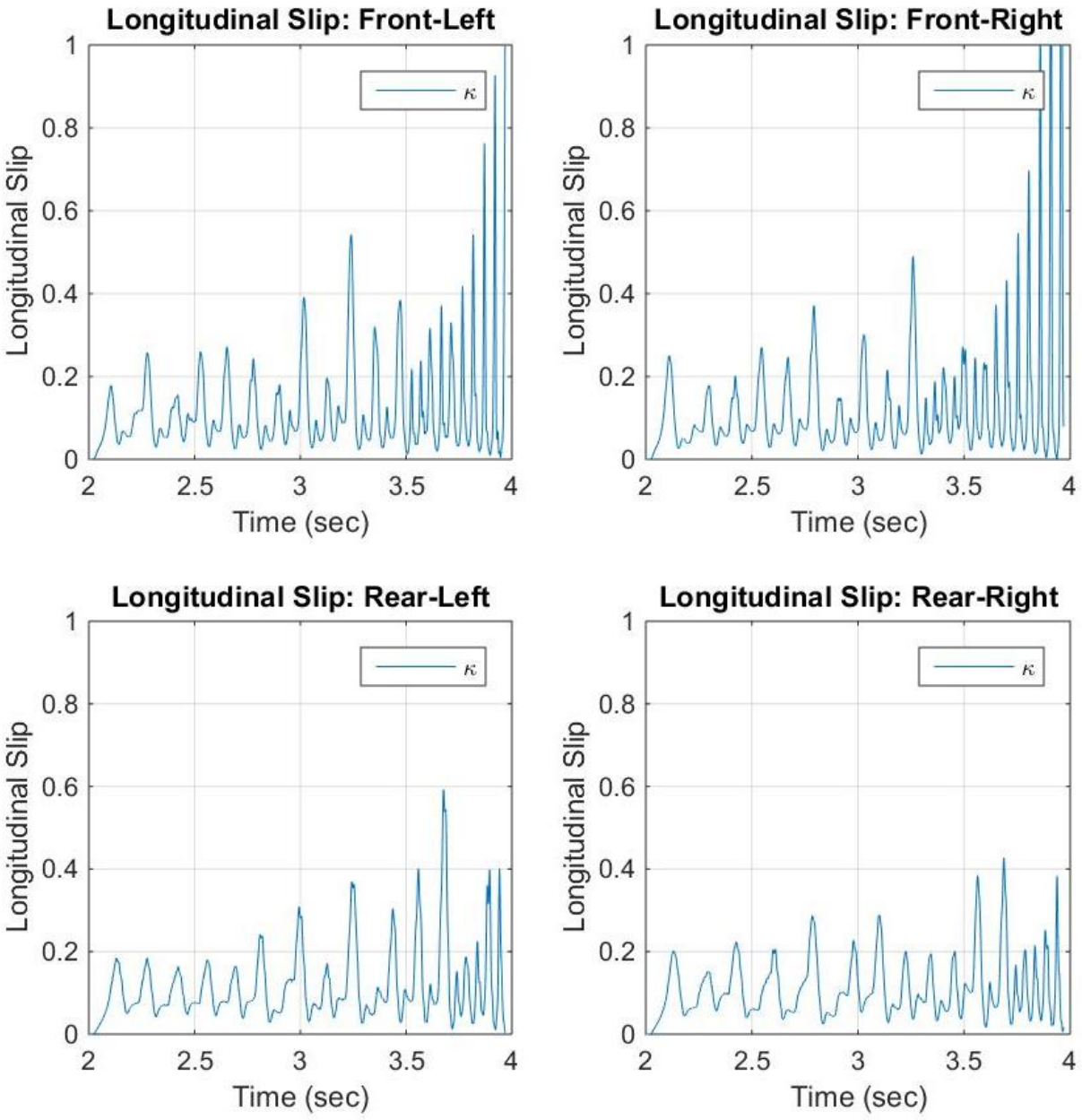

Figure 4.4: Simulation Results: Longitudinal Slip

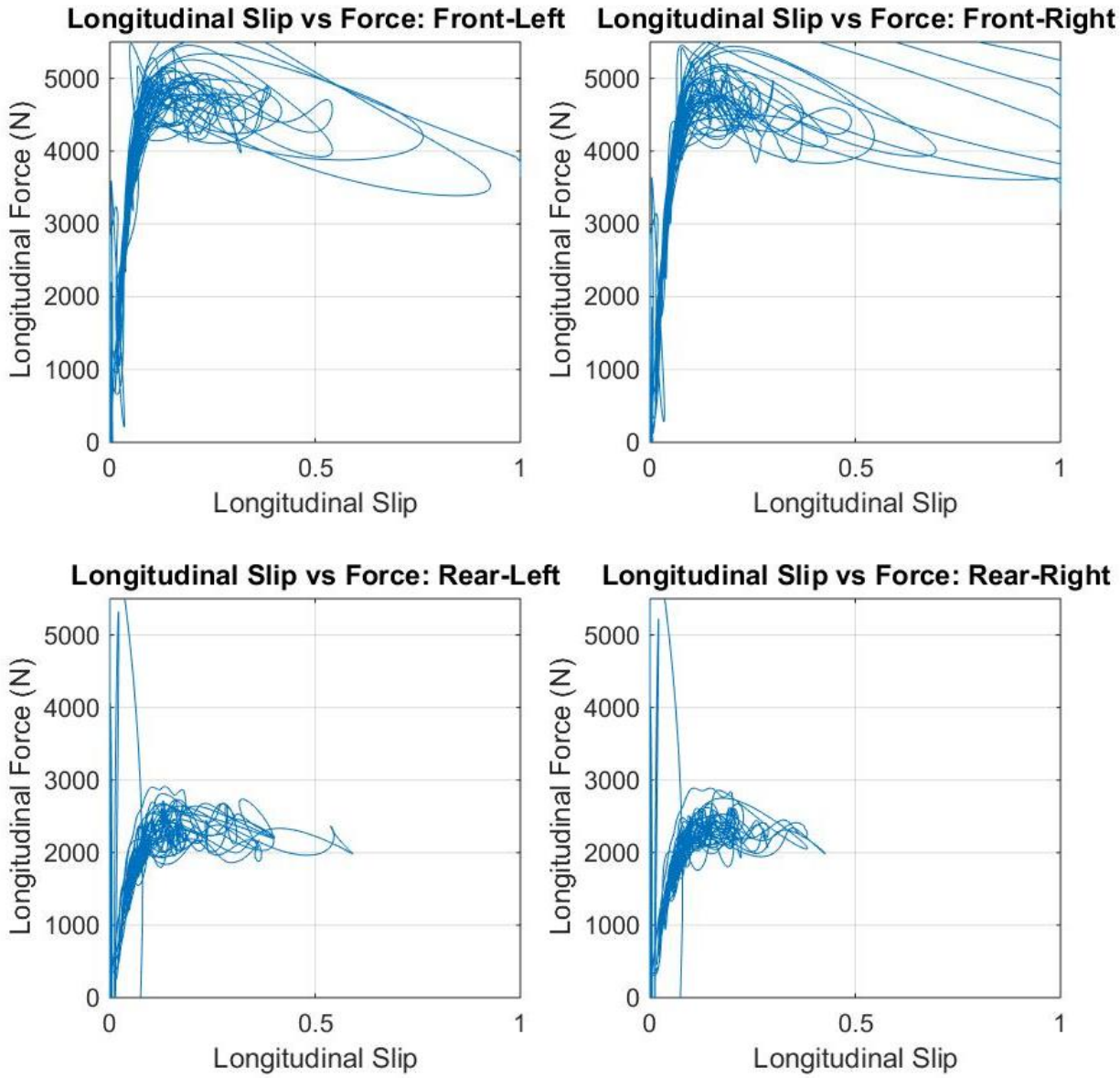

Figure 4.5: Simulation Results: Longitudinal Slip vs Braking Force

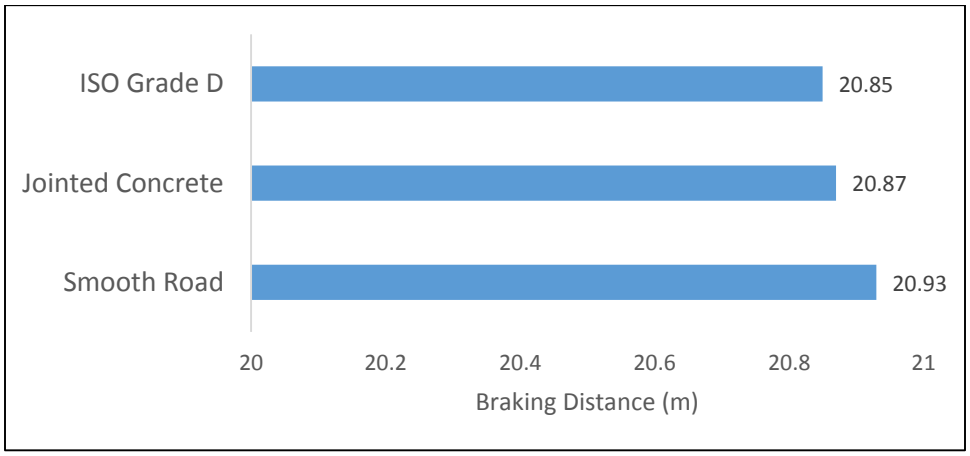

Figure 4.6: Simulation Results: Braking Distances

4.2 Validation

4.2.1 Introduction

Outdoor objective evaluations form an important part of both tire and vehicle design process since they validate the design parameters through actual tests and can provide insight into the functional performances associated with the vehicle. Even with the industry focused towards developing simulation models, their need cannot be completely eliminated as they form the basis for approving the performance predictions of any newly developed model. An objective test was conducted to measure the ABS performance of the tire simulation design tool. A sample vehicle and a set of tires were used to perform the tests- on a road with known profile. These specific vehicle and tire sets were selected due to the availability of the vehicle parameters, tire parameters and the ABS control logic. A test matrix was generated based on the validation requirements. The set of parameters to be measured were extracted from this test matrix to understand the demand on instrumentation, data

acquisition and post processing of the acquired data. A cost effective yet novel instrumentation circuit was designed to perform the measurements. These results as discussed here, were finally used to validate the performance of the developed vehicle simulation tool.

4.2.2. Test Details

As has been stated before, it is essential that the conditions for the validation test be matched exactly with those in the model. The following describes details of how this was ensured for the different aspects involved.

Tires:

The test tire was selected based on the availability of the experimental data and available tire parameters for modeling. The specification of the tire used was 205/60 R15 91V. The tire data was obtained from a trial version of TNO MF-Tool 6.1 [22] and was recorded using standard test procedures and experiment measurement conditions, as described in their documentation.

Vehicle

A sample vehicle was selected based on the availability of its data for modeling. The Kinematics and Compliances data of the vehicle was measured using a K&C Rig. The weight was measured using vehicle load cells and the center-of-gravity (CG) was calculated using the same load cells and lift-based measurement procedures. Other vehicle dimensions were recorded using standard measuring instruments.

Road

The test was performed on the ‘Smart Road’, which is a 2.2 mile controlled-access testing facility at the ‘Virginia Tech Transportation Institute (VTTI)’. Broadly, there were two types of road surfaces present on this road: a smoother surface and a relatively rougher surface. Profiles of these road surfaces were measured using vehicle mounted road profiling system as part of a previous research project. A sample 2-dimensional section of this profiled road has been shown in Figure 2.10, which has a gradient. Further, the test was performed on the straight section of the Smart Road, since the test involved straight line braking trials. This straight section of the track is seen to have a gradient of 2.3°. This was seen as a deviation from what has been considered in the models. In order to negate the effect of this gradient on test results, it was decided that the test was to be performed uphill as well as downhill for every test case. An assumption was made that an average of the test results for braking distances for Uphill and Downhill trials will be equal to the results obtained for the case if the road were to be flat.

4.2.3 Test Matrix

Before the test set-up could be designed, a test matrix was developed to understand the expectations from the validation test. Table 4.1 shows the developed test matrix. Using the individual parameters in the test matrix, the instrumentation set-up was then designed which is described in the next section.

Table 4.1: Test Matrix

	Conditions of Testing			
Parameters to be measured	Rough Surface Uphill	Rough Surface Downhill	Smooth Surface Uphill	Smooth Surface Downhill
Longitudinal Braking Distance	o	o	o	o
Longitudinal Velocity during Braking	•	•	•	•
Longitudinal Acceleration during Braking	•	•	•	•
o indicates standalone value requirements • indicates time function requirements				

4.2.4 Test Set-up

4.2.4.1 Position and Velocity Measurements

Brake Trigger

The brake pedal trigger was used to enable precise measurement of brake pedal application during the brake test. The trigger events are recorded at high frequencies of 100Hz. This high frequency provides a maximum of 10ms gap between the pedal application and when it is recorded. This time is then automatically included in the calculation to add the extra distance covered in this short time span. Figure 4.7 shows the brake pedal trigger that was used.

GPS

A 5V active GPS antenna was used for distance and velocity measurements. The GPS used was capable of measuring distance at the rate of 100Hz, with an accuracy of 0.05% and a resolution of 1cm. Likewise, the velocity was also measured at the rate of 100Hz, with an accuracy of 0.1km/h and a resolution of 0.01km/h. The GPS antenna which has a magnetic base was mounted on the vehicle roof, ensuring that at least 7 satellites were locked during testing at all times. Figure 4.7 shows the GPS antenna used.

VBox

The 3rd generation VBox was used for logging the test data from the brake trigger and the GPS. As stated earlier, the VBox is capable of recording the data at a rate of 100Hz. The logged data is directly stored onto a compact flash card to easily transfer to a PC and analyze using the VBox Tools software. While it simultaneously receives signals on brake triggering, position as well as velocity, it is easy to punch the brake trigger event to an exact location, at which point the velocity is also known. Using this as one reference and the stop velocity as another, the stopping distance can be calculated from the position of the vehicle, as all are plotted against time simultaneously. Figure 4.7 shows the VBox used.

Figure 4.7: Validation Measurement Instruments

4.2.4.2 Acceleration Measurements

Inertial Measurement Unit (IMU)

The Polulu MinIMU-9 v3, a 3 axis- accelerometer, gyroscope and magnetometer were used for the acceleration measurements during the brake tests. The measurement range of accelerometer was selected as ±2g and the sensitivity as 0.061mg/LSB, considering vehicular braking. Measurements for the roll, pitch, yaw, lateral acceleration and vertical acceleration were also obtained from this IMU. However, they were not considered for the current scenario of straight line braking. Figure 4.8 shows the IMU used. It consists of 5 pins for its connections, however only 4 of these are used for this application. (1) SCL- clock line, (2)SDA- data line, (3)GND- grounding and (4) VIN- power pin (to accept input voltage while using an external power source, which in this case is 5V). During testing, this IMU was mounted as close to the center-of-gravity as was practically possible to get the correct measurements.

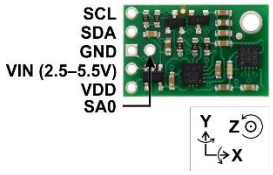

Figure 4.8: Inertial Measurement Unit (IMU) [23]-
Pololu Robotics and Electronics, © 2001-2015 Pololu Corporation,
https://www.pololu.com/ product/2468/pictures. Used under fair use 2015.

IMU Data Logger System In the manner that the VBox was used to log data from the GPS and brake trigger, a similar data logger system was necessary for logging data from the IMU. An Arduino coupled with a Data Logger Shield was used for

this purpose. The following sections describe how this system was designed and data logging was achieved:

Arduino

The Arduino that was used is a single board 8-bit micro-controller that consists of an open source hardware board with multiple analog and digital inputs along with the I2C serial bus. It is mainly used for communication and is designed for receiving inputs from sensors. This can then be coupled with another add-on module for recording this data. The 4 pins for clock, data, ground and power from the IMU are connected to the corresponding Arduino pins. The Arduino is powered with the help of 6 AA batteries through the power jack to generate the required power supply. The Arduino can be programmed to accept the data from the IMU by defining directories along with its time latencies i.e. the time delay between when the data is measured to when it is recorded.

Data Logger Shield

The Data Logger Shield is essentially used to save the data on any FAT16 or FAT32 formatted SD card. All of the recorded data are time-stamped using the built-in Real Time Clock (RTC). The RTC keeps the time going even when the Arduino is unplugged. It consists of a chip, crystal and a lifetime battery back-up. This behaves as an add-on attachment over the Arduino. A prototyping area is also provided over this shield. It is in this area that the IMU is mounted atop the stacking headers. Appropriate data writing can be ensured with the help of the same Arduino program. Figure 4.9 shows the IMU-Arduino-Data Logger Shield assembly that was used.

While portability of the IMU is an important factor, so is the sampling rate. Replacing the 6 AA batteries with small DC power supply could potentially improve the sampling rate from 100 Hz to 125 Hz. With the short duration tests that were

planned for this case, the voltage drop of the batteries was insufficient to slow the sampling rate. Another potential improvement would be to create a 3D printed case with variable external mounting options to allow faster IMU placement with different test rigs. Further, a long-term improvement would be to add an external switch to add a time-based trigger for easier post-test data processing.

An important advantage of using this IMU- Arduino setup is that it was developed for approximately a tenth of the cost of commercially available units with comparable accuracy. Further, with the help of this already developed circuit, the Arduino can be used for data acquisition of any other parameter like steering angle measurements, tire temperature measurements, etc. with slight modifications.

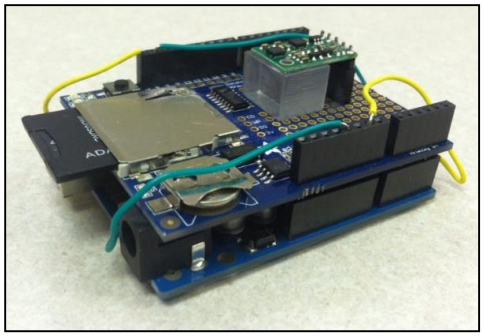

Figure 4.9: IMU-Arduino set-up

4.2.5 Validation Testing

To evaluate the straight line antilock braking of the vehicle, the initial velocity of the vehicle was considered to be 65 km/h (40.3 mi/h). Starting at this velocity, the vehicle was brought to a complete stop using ABS, simulating panic braking situations. As has been mentioned earlier, the gradient of the road was taken into consideration by performing the runs uphill and downhill, and then averaging the two test runs. Every run was performed 3 times to check for repeatability in the

results. The vehicle was maintained at the test weight throughout, with considerations of driver, co-driver and gas in the vehicle. This was confirmed after the test when the vehicle was weighed again. Standard testing protocols were followed while testing. Quick checks were made after each run if the data was being recorded appropriately. A test log was maintained to make critical notes such as what test was performed on which run- along with a time stamp, so as to make data processing easier. With two different circuits recording data simultaneously, it was made sure that data miss-match does not occur. Syncing the times of these two clocks precisely with each other ensured this. It was made sure that an experienced driver was performing the test. The most critical aspects of driving were maintaining the initial speed up to the required mark and to simulate the panic braking condition with a completely depressed brake pedal. A post-test analysis showed that the initial test speed error was maintained at lower than 1.1% of the originally required speed for all test runs. This confirmed that the variations due to human factors were kept to a minimum, so as not to affect the test results in any manner. The tests were performed in favorable environmental conditions. Wind speeds were ensured to be lower than 10-15mph so as not to have a considerable effect on the vehicle to affect its braking performance. In addition to the above mentioned details, all standard safety procedures were followed while performing these tests.

4.2.6 Results and Comparison

4.2.6.1 Braking Distances

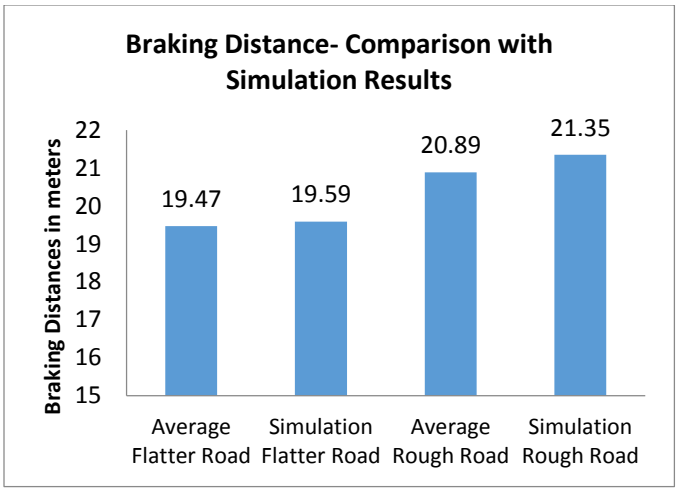

Figure 4.10: Braking Distance: Simulation vs Validation

Figure 4.10 shows a comparison of the braking distances for the validation results vs simulation results. The coefficients of friction used for the two sets of simulation were 0.982 for the flatter road and 0.919 for the rougher road as obtained from VTTI.

1. Simulation comparisons have been presented for the two road cases. As stated earlier, the uphill and downhill results have been averaged out.
2. For the flatter road, a braking distance of 19.47m was observed. The simulation result of 19.59m lies within 0.6% of the validation result.
3. For the rougher road, a braking distance of 20.89m was observed. The simulation result for this road profile was 21.35m. This was within 2.2% of the validation result.
4. For the simulation tool that was developed, a variation of 3-5% was considered to be within tolerable limits considering current similar commercially available tools as benchmark. This was mainly due to the fact that the simulation tool in its current form, considers a constant coefficient of friction throughout the braking simulation. Further, temperature changes in the tire contact patch have not been considered in the simulations. These two factors are assumed to have significant effects on the braking results predicted.

With that, 0.6% and 2.2% were considered to be close correlations. Model development for the above mentioned factors is currently under progress, and a closer correlation with the test results should be observed once they are factored in.

5. Upon closer observation, it is seen that the braking distance for the rougher road is higher than that for the flatter road, for both- simulation and test results. This shows that the rougher road tends to set vibrations in the tires, which reduces the tire's capability to perform well under ABS conditions.

4.2.6.2 Braking Velocities

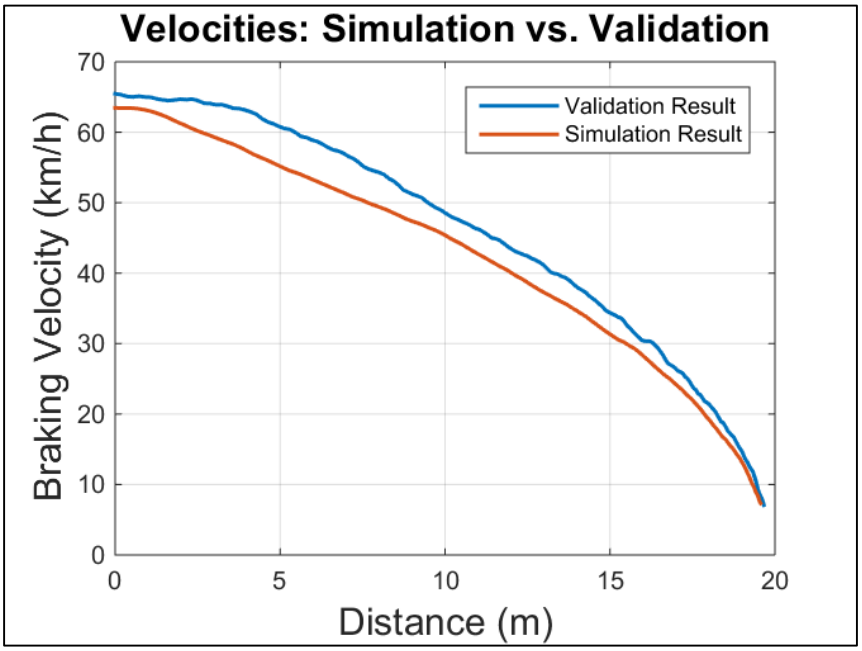

Figure 4.11: Braking Velocity: Simulation vs Validation

1. Figure 4.11 shows a comparison of the distribution of Velocity vs Distance between the test and simulation. To avoid the effect of roll-back (backward

jerk given by the vehicle when it stops completely) and initial speed variations from affecting the braking distance results, measurements were considered between two fixed speeds which would lie between the end limits. In line with this, the stop speed for calculations was considered as 7.2km/h. Braking distance was calculated as the difference between the distance values at these two fixed speeds from the plot.

2. The plot shows the simulation result traces the test result closely. A correlation coefficient of 0.9975 is observed between the two plots. This is considered as a highly correlated data. Further, a second derivative with respect to time of this plotted data gives a more accurate estimate of the correlation. This correlation has been verified with the help of acceleration plots in the next section.

4.2.6.3 Braking Decelerations

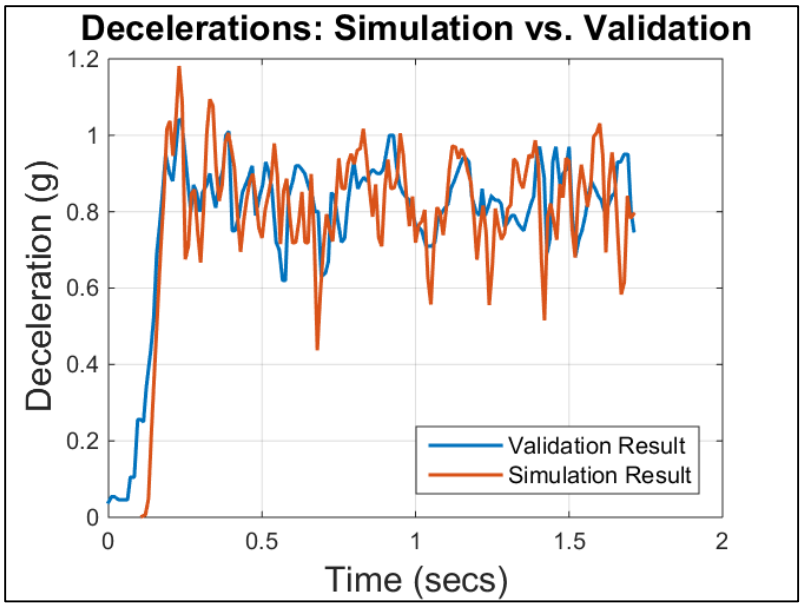

Figure 4.12: Braking Deceleration: Simulation vs Validation

1. Figure 4.12 shows the comparison between the acceleration plots obtained from the test and simulation results. This plot has been truncated to the region that does not involve the development and reduction of this deceleration in order to have detailed views. Here, positive acceleration is considered for braking.
2. It is seen that the simulation result generally has the same trend as the validation test result.
3. A correlation coefficient of 0.9239 was observed between the simulation data and the validation data.
4. Fluctuations in the acceleration plots indicate jerks in the longitudinal direction. These jerks are a result of the ABS controller in operation, as it increases and decreases brake pressure depending on the slip at the wheels.

Chapter 5:

Conclusions

The following provides a summary of the work that was done as part of developing the simulation tool:

- The simulation tool developed was capable of predicting the straight line antilock braking performances of a vehicle
- The rigid-ring tire model was used for the simulations which is capable of analyzing the dynamic performance of tires up to a frequency of 100Hz required for the application of antilock braking as well as short wavelength disturbances from the road
- An antilock braking model developed in Simulink was utilized to excite the tire at the frequency and magnitude comparable commercially available systems
- The tire and ABS models were integrated with CarSim®, which enables easy implementation of vehicles for simulation
- Vehicle data of an actual vehicle obtained from a K&C machine was implemented in CarSim® in order to compare Simulation results with the validation data.
- Predictions of braking distance, velocities, wheel slip and braking torques were presented. A range of road profiles were used for the simulations and their performances were compared.

- A good computation efficiency was obtained for the simulation tool when compared to other tools like finite element modeling packages.
- Validation tests were performed on the track to obtain braking test data from the same set of vehicle, tires and brakes that were used for the simulation. The V-Box was used for obtaining the position and velocity measurements and an in-house developed accelerometer was used to obtain the deceleration measurements.
- Braking distance results correlated to within 0.6% and 2.2% for the flatter and rougher road respectively. Velocity, when plotted against distance, gave a correlation coefficient of 0.9975 between the simulation and validation results. Acceleration simulation results were also seen to have a close correlation with validation. Thus, the simulation results were successfully validated.

Recommendations for Future Work:

- Building the simulation tool as a standalone package using C/C++ that can be deployed on any platform
- Parameterization of the ABS model to allow for adjustments in wheel acceleration thresholds and compatibility with different simulation time-steps
- Implementation of a magic formula based approach to calculate steady state tangential forces in the contact patch instead of a brush model
- Validate the simulations of the quarter car with an ABS system through Hardware-In-the-Loop (HIL) simulations
- Estimate the dynamic stiffness of the sidewall by fitting the model response to experimental data obtained from high-speed cleat tests

References

1. Jorge Segers ‘Analysis Techniques for Race Car Data Acquisition’, SAE International, 2014.
2. Peter W.A. Zegelaar, ‘The dynamic response of tires to brake torque variations and road unevenness’, Ph.D. thesis, Delft University of Technology, Netherlands, 1998.
3. Srikanth Sivaramakrishnan, ‘Discrete Tire Modeling for Antilock Braking System Simulations’, M.S. thesis, Virginia Tech, Blacksburg, VA, 2013.
4. ‘The Pneumatic Tire’- National Highway Traffic Safety Administration, U.S. Department of Transportation, February 2006.
5. Hans Pacejka, ‘Tire and Vehicle Dynamics’, Elsevier Ltd., 2012.
6. Taheri, Sh., Sandu, C., Taheri, S., Pinto, E., Gorsich, D. ‘A Technical Survey on Terramechanics Models for Tire-Terrain Interaction Used in Modeling and Simulation of Wheeled Vehicles’, J. of Terramechanics, Vol. 57, pp. 1-22 (22).
7. Ayman A. Aly, El-Shafei Zeidan, Ahmed Hamed, Farhan Salem, ‘An Antilock-Braking Systems (ABS) Control A Technical Review’, Intelligent Control and Automation 2011.
8. J. Song, H. Kim and K. Boo, ‘A study on an Anti-Lock Braking System Controller and Rear-Wheel Controller to Enhance Vehicle Lateral Stability’,

Proceedings of the Institution of Mechanical Engineers, Part D: Journal of Automobile Engineering, Vol. 221 No. 7, 2007, pp. 777- 787. doi: 10.1243/09544070JAUTO225.

9. F. Jiang, ‘An Application of Nonlinear PID Control to a Class of Truck ABS Problems’, Proceedings of the 40th IEEE Conference on Decision and Control, Orlando, 2000, pp. 516-521.
10. R.-G. Wang, Z.-D. Liu and Z.-Q. Qi, ‘Multiple Model Adaptive Control of Antilock Brake System via Back stepping’, Proceedings of 2005 International Conference on Machine Learning and Cybernetics, Guangzhou, 2005, pp. 591-595.
11. W. Ting and J. Lin, ‘Nonlinear Control Design of Anti-lock Braking Systems Combined with Active Suspensions’, Technical Report of Department of Electrical Engineering, National Chi Nan University, 2005.
12. B. Ozdalyan, ‘Development of A Slip Control Anti-Lock Braking System Model’, International Journal of Automotive Technology, Vol. 9, No. 1, 2008, pp. 71-80. doi:10.1007/s12239-008-0009-6.
13. W. K. Lennon and K. M. Passino, ‘Intelligent Control for Brake Systems’, IEEE Transctions on Control Systems Technology, Vol. 7, No. 2, 1999, pp. 188-202. doi:10.1109/87.748145.

14. Jaehoon Lee, Jonghyun Lee, Seung-Jin, Heo, 'Full vehicle dynamic modeling for Chassis Control', FISITA, F2008-SC-021.
15. A. Schmeitz, 'A Semi-Empirical Three-Dimensional Model of the Pneumatic Tyre Rolling over Arbitrarily Uneven Road Surfaces', Ph.D. thesis, Delft University of Technology, 2004.
16. N. Ding, W. Wang, G. Yu, W. Zhang, X. Xu, D. Nenggen, W. Weida, Y. Guizhen, and Z. Wei, 'Research and Validation of the Adaptive Control Strategy for ABS Based on Experimental Knowledge' Automotive Engineering, vol. 31, no. 1, 2009.
17. Timothy Paul Wagner, 'The Mechanical Design of a Suspension Parameter Identification and Evaluation Rig (SPIdER) for Wheeled Military Vehicles' M.S. thesis, The Ohio State University, 2011.
18. AB Dynamics, 'SPMM 5000, Outline Specification – SP20016 issue 2' available online at http://www.abd.uk.com/upload/files/2014-09-10_17-08-17_Sp20016%20i2%20SPMM%205000%20Outline%20Specification.pdf.
19. CarSim® Manuals, 'Vehicle Suspension Models', Mechanical Simulation Corporation, 2005-2015.
20. Michael W. Sayers, Steven M. Karamihas, 'The Little Book of Profiling', The Regent of the University of Michigan, September 1998.

21. CarSim® Manuals, ‘Model Screens’, Mechanical Simulation Corporation, 2005-2015.
22. TNO Automotive, ‘MF-Tyre/MF-Swift 6.1.2.1 Help Manual’, 2012.
23. Pololu Robotics and Electronics, © 2001-2015 Pololu Corporation, https://www.pololu.com/ product/2468/pictures.